Petrogenesis of the chromitite body from the Cerro Colorado ophiolite, Paraguaná Peninsula, Venezuela

Petrogénesis del cuerpo de cromitita de la ofiolita del Cerro Colorado, península de Paraguaná, Venezuela

David J. **Mendi**[1,2], José María **González-Jiménez**[1,*], Joaquín Antonio **Proenza**[3], Franco **Urbani**[2], Fernando **Gervilla**[1,4]

[1] Departamento de Mineralogía y Petrología, Facultad de Ciencias, Universidad de Granada, Avenida. Fuentenueva s/n, 18002 Granada, Spain.

[2] Universidad Central de Venezuela, Facultad de Ingeniería, Escuela de Geología, Minas y Geofísica, Caracas 1051, Venezuela.

[3] Departament de Mineralogia, Petrologia i Geologia Aplicada, Facultat de Ciències de la Terra, Universitat de Barcelona, 08028 Barcelona, Spain.

[4] Instituto Andaluz de Ciencias de la Tierra (IACT), CSIC-UGR, Avda. de las Palmeras 4, 18100 Armilla, Granada, Spain.

* Corresponding author: (J.M. González)
jmgonzj@ugr.es

ABSTRACT

Ultramafic-mafic rocks of ophiolitic affinity crop out along the Venezuelan Caribbean region. They have been interpreted as remnants of the oceanic lithosphere of the Caribbean volcanic arc (135-70 Ma) as well as relics of proto-Caribbean oceanic lithosphere (Upper Jurassic-Lower Cretaceous) related to Pangea's break-up. The Cerro Colorado ophiolite, located in the Paraguaná Peninsula, together with the case of the Cordillera de la Costa in north-central Venezuela, are a unique case of these Venezuelan ophiolites containing chromitite bodies. However, the petrogenesis of such a mafic-ultramafic complex and associated chromite ore remains are unknown to date. To advance our understanding of chromite ores in the Caribbean region, the genesis of the Cerro Colorado chromitite body is challenged. The Cerro Colorado chromitite body is characterized by a low-Cr content [Cr# =Cr/ Cr+Al= 0.44-0.60] and a distribution of trace elements in chromite as is typical of high-Al chromitites found in the shallower portions of the petrological Moho Transition Zone of Mesozoic ophiolites. The calculated melts in equilibrium with chromite forming this high-Al chromitite body are back-arc basin basalts. These melts were extracted after ~20 % partial melting of moderately depleted peridotites, which resulted in the precipitation of high-Al chromitite relatively impoverished in PGE (≤ 100 ppb total PGE). A comparison of the geochemical signatures of minor and trace elements in chromite and bulk-PGE contents of the Cerro Colorado chromitite with those of other known chromitites in the peri-Caribbean ophiolites show certain similitude with those high-Al described in the Moa-Baracoa ophiolite in eastern Cuba. The obtained results allow us to suggest that the ultramafic rocks of the Cerro Colorado and the chromitite body associated with it are closely related to the formation of a back-arc basin developed between ca. 125-120 Ma in the rear of the Great Antilles Arc.

Keywords: Ophiolite, chromite deposit, platinum-group elements, Caribbean, Venezuela.

RESUMEN

El margen caribeño de Venezuela se caracteriza por la presencia de algunos afloramientos de rocas máficas y ultramáficas de afinidad ofiolíca. Dichas rocas se han intepretado como fragmentos de la litosfera oceánica del Arco volcánico Caribeano (~135-70 Ma) así como relictos de la litosfera oceánica del proto-Caribe (Jurásico Superior-Cretácico Inferior) relacionados con la ruptura de Pangea. La ofiolita de Cerro Colorado, localizada en la Península de Paraguaná es, conjuntamente con el caso de la Cordillera de la Costa en la parte centro norte de Venezuela, el único caso de esas ofiolitas Venezolanas que contienen cuerpos de cromititas. Sin embargo, se desconoce aún la petrogénesis de dichos complejos de rocas máficas y ultramáficas. Con el objeto de avanzar en el estado del conocimiento de la génesis de menas de cromita en la región del Caribe, en este trabajo se aborda el estudio de la génesis del cuerpo de cromitita de Cerro Colorado. El cuerpo de cromitita de Cerro Colorado está constituido esencialmente por cromita con bajo contenido en Cr [Cr# =Cr/ Cr+Al= 0.44-0.60] y una distribución de elementos trazas similar a la descrita en otras cromititas con alto contenido en Al documentadas en las zonas más someras de la Zona de Transición de la Moho petrológica de otras ofiolitas de edad Mesozoica. Los fundidos calculados en equilibrio con la cromita que forma este cuerpo de cromititas con alto Al son basaltos de trasera de arco. Estos fundidos fueron extraídos de una mantélica formada por peridotitas empobrecidas como resultado de tasas de fusión parcial de ~20 %, lo que dió lugar a la precipitación de cromititas con alto Al relativamente empobrecidas en EGP (≤ 100 ppb suma total de EGP). Una comparación de las firmas geoquímicas de los elementos menores y trazas en la cromita y contenidos de EGP obtenidos a partir del análisis de muestras de roca total de la cromitita de Cerro Colorado con otras cromititas documentadas en el manto de ofiolitas peri-Caribeñas muestra cierta similitud con aquellas altas en Al descritas en la ofiolita de Moa-Baracoa en Cuba oriental. Los resultados obtenidos nos permiten sugerir que las rocas ultramáficas de Cerro Colorado y el cuerpo de cromitita que éstas albergan están íntimamente relacionados con la formación de una cuenca de retro arco desarrollada en un el intervalo temporal 125-120 Ma en la trasera del Arco de las Antillas Mayores.

Palabras clave: Ofiolita, depósito de cromita, elementos del grupo del platino, Caribeño, Venezuela.

1. Introduction

A chromitite is a very peculiar case of magmatic rock where chromite is the predominant mineral (> 80 % vol). This type of rock is usually associated with mafic and ultramafic rocks, specifically peridotites and their serpentinized equivalents, with two main styles of ores distinguished by their geological setting: (1) stratiform or Bushveld-type chromitite associated with layered mafic intrusions (*e.g.*, Mukherjee *et al.*, 2017; Latypov *et al.*, 2017;

Mathez and Kinzler, 2017) and (2) "podiform" or ophiolitic chromitite hosted in fossil oceanic lithosphere (Leblanc and Nicolas, 1992; González-Jiménez *et al.*, 2014; Arai and Miura, 2016). In the last few decades the interest for chromitite has greatly been increased because their intriguing genesis (*e.g.*, Rollinson, 2016; O'Driscoll and Van-tongeren, 2017) and economic interest as a unique source of the metal chromium and potential target for the recovery of the critical raw metal platinum-group elements (O'Driscoll and González-Jiménez, 2016; Mudd *et al.*, 2018).
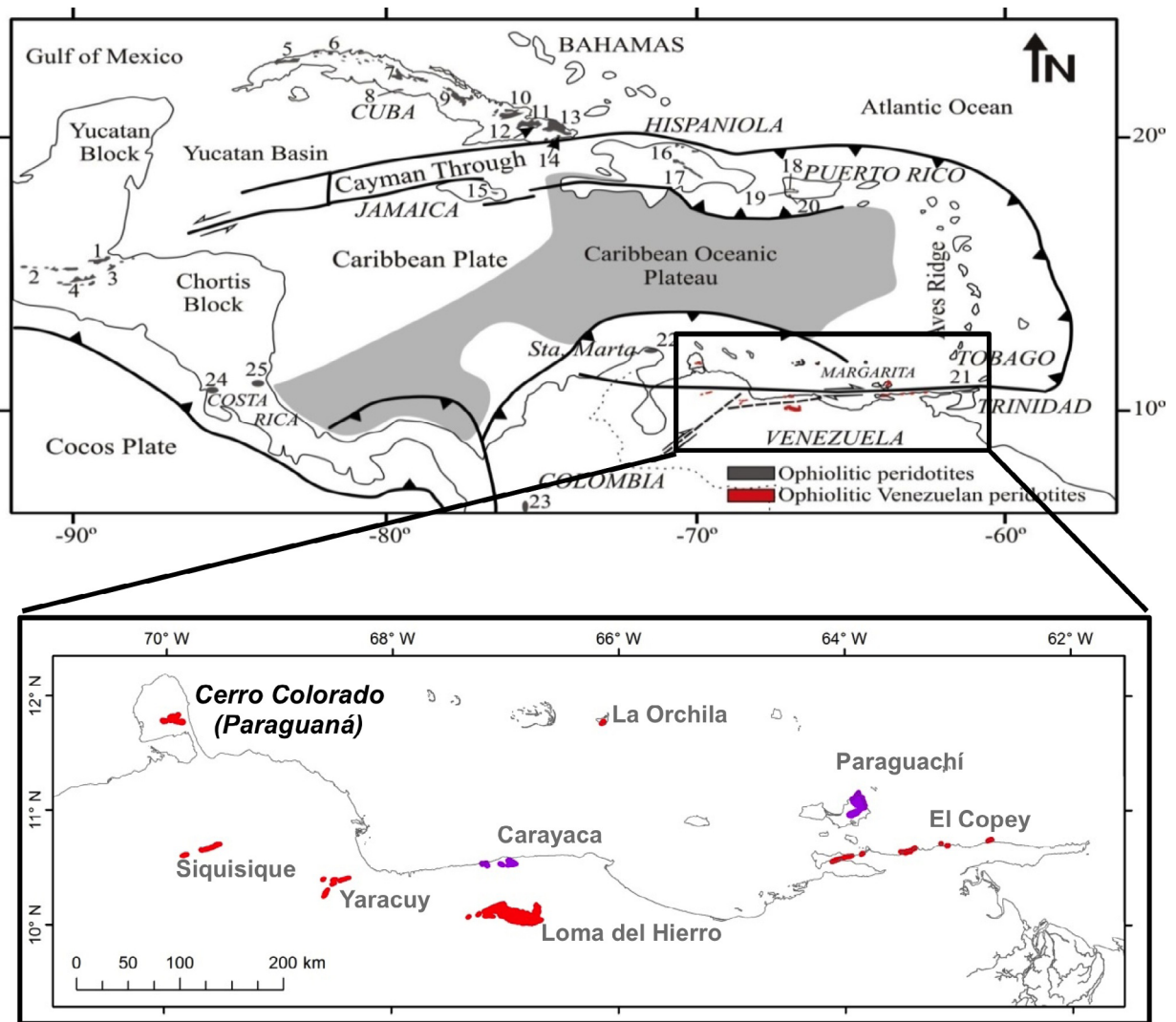

Figure 1 (a) Distribution of ophiolite-related ultramafic rocks around the margins of the Caribbean Plate (from Lewis *et al.*, 2006): 1) Sierra de Santa Cruz, 2) Baja Verapaz, 3) Juan de Paz, 4) Grupo El Tambor, 5) Cajálbana, 6) Habana-Matanza, 7) Villa Clara, 8) Escambray, 9) Camagüey, 10) Holguín, 11) Mayarí-Cristal, 12) Alto de La Corea, 13) Moa-Baracoa, 14) Sierra del Convento, 15) Arntully, 16) North Coast Belt, 17) Loma Caribe, 18) Monte del Estado, 19) Río Guanajibo, 20) Bermeja, 21) San Souci, 22) Serpentinitas de Cabo de la Vela (Guajira), 23) Dunita de Medellín, 24) Santa Elena, 25) Río San Juan. Northern Venezuelan ophiolites are marked in red in (a) and zoomed in (b).

In Latin America, chromitites of the *stratiform-type* have been exclusively reported from large layered intrusions within Archean cratons and Neoproterozoic continental crust in Brazil (*e.g.*, Ferreira-Filho *et al.*, 2002). In contrast, chromitites of the *ophiolitic-type* are relatively frequent in many of the ophiolites widespread throughout the whole continent in North, Central and South America. The latters have been mainly found in suprasubduction-zone ophiolites (SSZ) corresponding to oceanic lithosphere that preserve an evolution or transition from back-arc to fore-arc environments or vice versa (*i.e.*, MORB-island arc tholeiite–boninite sequence of igneous activity). Most of these chromitites were already exploited for chromium since middle 20th Century, although some ophiolites with strong potential for chromite deposits still remain underexplored. Examples of ophiolitic chromitites associated with SSZ ophiolites in North Latin America include those metamorphosed ones of Paleozoic age reported from Tehuitzingo and Loma Baya in Mexico (Proenza *et al.*, 2004a; González-Jiménez *et al.*, 2017a; Colás *et al.*, 2017; Farré-de-Pablo *et al.*, 2019), and the unaltered Triassic ophiolites from the Mexican Baja California (*i.e.*, Puerto Nuevo; Vatin-Perignon *et al.*, 2000; González-Jiménez *et al.*, 2017b). In South Latin America, chromitite are known from the metamorphosed ophiolites of Neoproterozoic age of the Eastern Papean Ranges (Los

Congos and Los Guanacos; Proenza *et al.*, 2008; Colás *et al.*, 2016), the Paleozoic ultramafic massifs of Tapo in Peru (Tassinari *et al.*, 2011; Colás *et al.*, 2017) and La Cabaña in Chile (Barra *et al.*, 2014; González-Jiménez *et al.*, 2016), and the Permian-Triassic Medellin Metaharzburgitic Unit in the Central Cordillera of Colombia (Proenza *et al.*, 2004b; Correa-Martínez, 2007). A remarkable suite of relatively well-preserved chromite deposits cropping out in the (peri)-Caribbean region in North, Central and South America are associated ophiolites corresponding to remnants of the oceanic lithosphere of Late Jurassic–Early Cretaceous. These include the chromitite deposits of Baja Verapaz in Guatemala (Thayer, 1946), Siuna in Nicaragua (Flores *et al.*, 2007; Baumgartner *et al.*, 2004), Santa Elena in Costa Rica (Zaccarini *et al.*, 2011), Northen Cuban ophiolite belt that includes a set of allochthonous massifs (Cajálbana, Habana-Matanzas, Villa Clara, Camagüey, Holguín, Mayarí-Baracoa) distributed along more than 1000 km in the mainland island of Cuba (Thayer, 1946; Proenza *et al.*, 1999, 2018; Gervilla *et al.*, 2005; González-Jiménez *et al.*, 2011a), and Loma Peguera in the Dominican Republic (Proenza *et al.*, 2007).

This paper provides the first scientific report of a chromitite body associated with the Cerro Colorado Ophiolite, in the Paraguaná Peninsula, in the northern part of Venezuela. Méndez (1960)
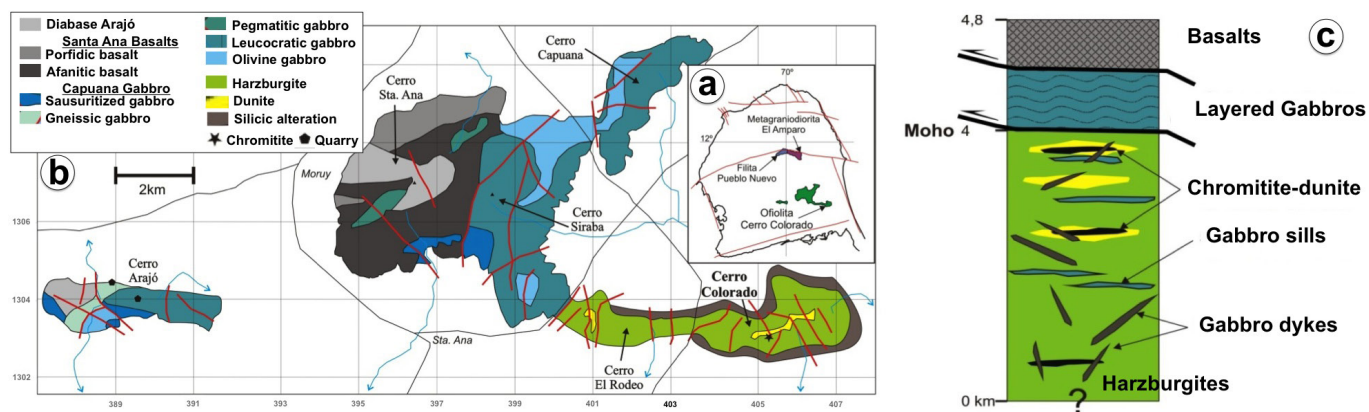

Figure 2 (a) Geological map of the studied area in the northern part of the Pagaguaná Peninsula along the north coast of Venezuela showing the location of the chromite body studied herein (b) and the pseudostratigraphy of the Cerro Colorado ophiolite (c). The map and the stratigraphic column are adapted from Mendi and Rodríguez (2006).
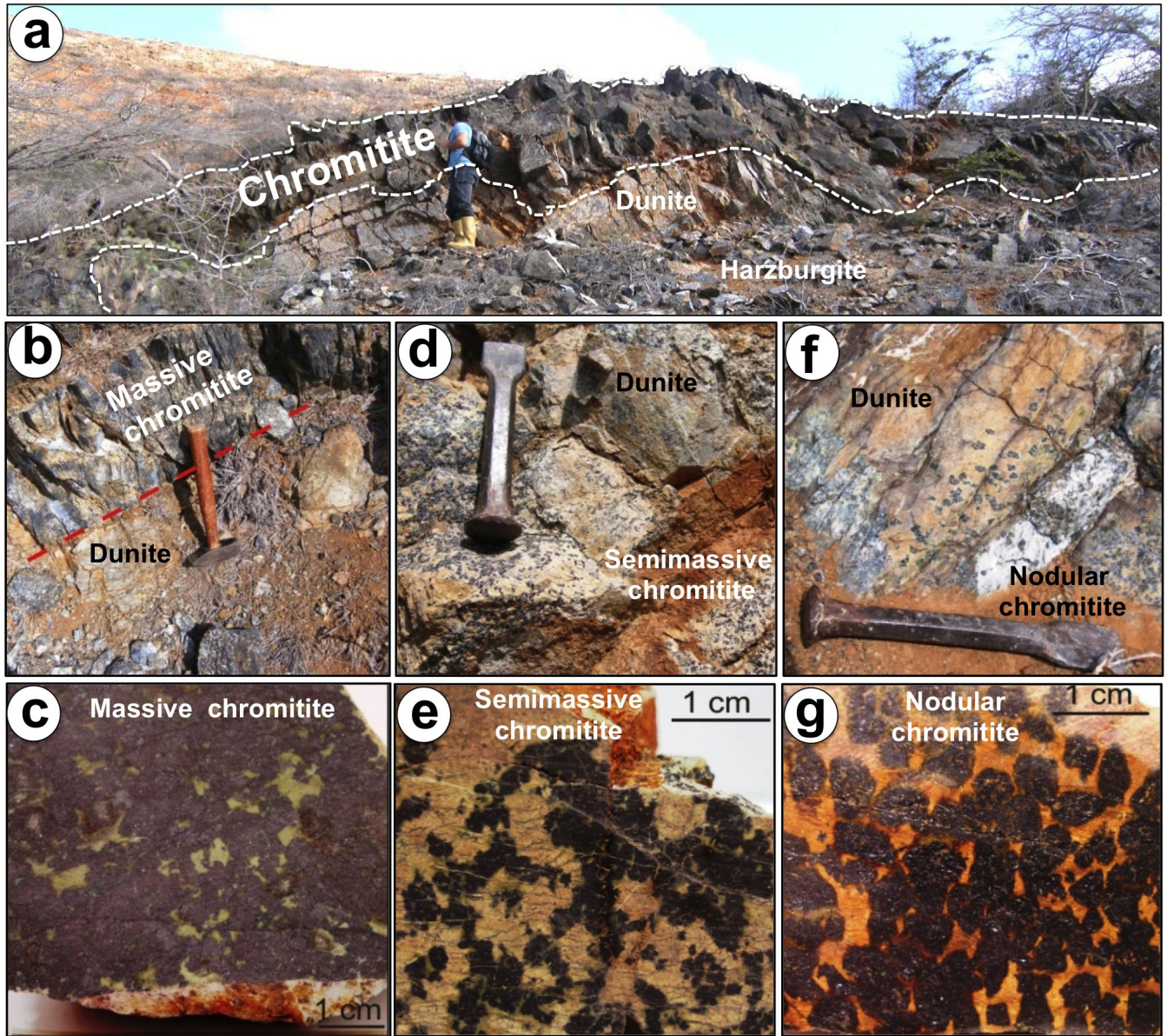
INTRODUCTION

Petrogenesis of a chromitite body from Venezuela

Figure 3 Photographs showing morphologies and textures of the Cerro Colorado chromitite body. (a) Chromitite pod within dunite enclosed in harzburgite. (b-c) Massive chromitite showing sharp contact with enclosing dunite. (d-e) Semi-massive chromitite hosted in dunite. (f-g) nodular chromitite hosted in dunite.

investigated for the first time this chromitite body, reporting the exact location, morphology, size and field relations of this chromitite body; however he did not provide any geochemical data nor an interpretation on its petrogenesis. This paper presents and discusses whole-rock PGE data on this chromitite and novel micro-analytical data, obtained using electron-microprobe and *in situ* ablation technique, for a suite of key minerals and elements of the chromitite and host peridotites. These data are integrated with field information and compared with recently published experimental and empirical data on ophiolitic chromitites, in order to identify the nature of the parental melt of the chromitite and, indirectly, precisely constrain the tectonic setting of their emplacement in the geological framework of the (peri)-Caribbean region.

2. Geological setting and chromitite

2.1. PERI-CARIBBEAN OPHIOLITES IN THE NORTHERN COAST OF VENEZUELA

Jurassic-Cretaceous ophiolitic rocks crop out along three margins of the Caribbean plate (Figure 1). These have been interpreted as relicts of pro-to-Caribbean oceanic lithosphere formed after Pangea's break-up or remnants of the oceanic lithosphere related to the origin and evolution of the Caribbean volcanic arc (135-70 Ma). In the northern coast of Venezuela, these "ophiolitic" sutures comprise, from east to the west, the ophio-

Figure 4 Photographs of thin sections of chromitite and photomicrographs (reflected light) showing main textural types in the Cerro Colorado chromitite body. (a) Massive chromitite, (b) Semi-massive chromitite, (c) nodular chromitite. Keys: Chr: chromite, Serp: serpentine.

lites of the El Copey (Araya-Paria; Alvarado, 2010; Petrásh and Revanales, 2010), Paraguachí (Margarita Island; Rekowski and Rivas, 2006; Maresch *et al.*, 2009), La Orchila (Cáceres, 2016), Carayaca (Cordillera de la Costa; Sisson *et al.*, 1997; Urbani, 2018), Loma del Hierro (Caucagua-El Tinaco; Baquero *et al.*, 2013; Urbani, 2018), Yaracuy (San Felipe; Bellizzia and Rodríguez, 1976), Siquisique (Rodríguez and Muñoz, 2009; Kerr *et al.*, 2012) and Cerro Colorado (Paraguaná; Santamaría and Schubert, 1974; Mendi and Rodríguez, 2006; Baquero *et al.*, 2013) (Figure 1).

The Cerro Colorado ophiolite, the subject of this paper, crops out in the southern part of the Paraguaná Peninsula corresponding to the most important topographic highs in the region (Figure 1, 2a and 2b). The ophiolite sequence consists, from bottom to the top (Figure 2c; Mistage, 1989; Mendi and Rodríguez, 2006), of strongly tectonized mantle clinopyroxene-bearing harzburgite containing sills and dykes of pyroxenites and gabbroic rocks (diabase, gneissic and pegmatitic gabbro, leucogabbro, olivine-bearing gabbro, norite and troctolite, anorthosite) as well as dunite lenses occasionally containing impregnation of clinopyroxenes and chromitite ore. This section of upper mantle rocks is tectonically overlain by a sequence of layered gabbros and extrusive basaltic and hypabyssal gabbroic rocks.
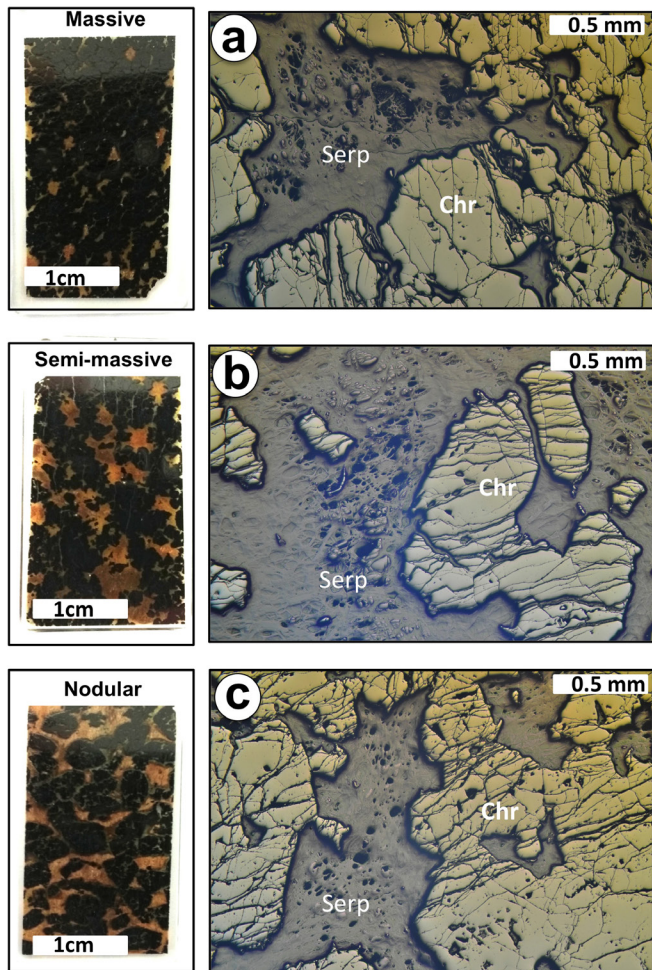
2.2. THE CHROMITITE BODY OF CERRO COLORADO OPHIOLITE

The chromitite body investigated in this work is located at the Cerro Colorado, west to the Santa Ana Village, in the southern part of the Paraguaná Penisula, Falcon state in north Venezuela (Figure 2a to 2c). The chromitite is a podiform-like body of 4 x 12 m that extends over about 45 m long trending N50°E and dipping 15° to the northwest concordantly with the host dunite-harzburgite and a sill of gabbro (Figure 3a). It is strongly fractured and locally intruded by peridotite dykes. The body chiefly consists of massive chromitite, although semimassive, disseminated and nodular-textured ores are also found in the external parts of the

Table 1. Ranges of major elements in chromite from the Cerro Colorado chromitite body and enclosing peridotites. Values of major elements are shown in wt.% as obtained from electron-microprobe.

	Massive n = 75		Semimassive n = 30		Disseminated n = 15		Nodular n = 15		Dunite n = 30		Harzburgite n = 15	
	Max	Min	Max	Min	Max	Min	Max	Min	Max	Min	Max	Min
SiO_2	0.06	0	0.06	0	0.23	0	0.04	0	0.63	0	0.04	0
Al_2O_3	25.37	21.01	25.54	24.49	31.2	29.59	31.16	29.61	27.55	19.25	25.41	21.84
Cr_2O_3	46.15	41.63	43.18	41.19	37.32	36.27	40.12	36.41	41.86	34.6	44.34	40.24
FeO	13.43	12.05	12.6	11.81	11.44	10.66	15.44	11.52	20.82	15.2	16.03	14.25
Fe_2O_3	4.27	2.9	4.47	3.26	3.84	3.05	3.87	0	10.97	6.07	4.85	4.04
MgO	15.34	14.14	15.56	14.82	16.82	15.96	16.19	12.84	13.64	8.83	13.97	12.38
TiO_2	0.35	0.1	0.37	0.18	0.19	0.1	0.18	0.1	0.31	0.19	0.1	0
Cr#	0.6	0.52	0.54	0.52	0.46	0.44	0.48	0.44	0.59	0.46	0.58	0.52
Mg#	0.69	0.65	0.7	0.68	0.74	0.72	0.71	0.6	0.62	0.43	0.63	0.58

orebody (Figure 3b to 3f). The contact between massive chromitite and dunite is usually sharp (Figure 3b) but in some zones of the body there is gradation from massive chromitite towards semimassive, disseminated and nodular-textured ore (Figure 3d and 3e). In the northern part of the chromitite body, there is a satellite vein made up of disseminated and nodular chromitite (up to 3 m long) emerging irregularly from the main body and penetrating into the host dunite.

3. Petrography

3.1. CHROMITITE

Massive chromitite (> 80% vol. chromite) forms the main part of the ore body and consists of aggregates of strongly fractured anhedral chromite (1-5 mm in size) grains. In some of the samples, the interstitial silicate matrix (representing < 20 vol.%) consists of olivine partially transformed to mesh lizardite cross-cut by late chrysotile veins (Figure 4a). Semimassive samples (70-80 vol. % chromite) consist of anhedral crystals of chromite of up to 4 mm across embedded in a serpentine matrix, whereas nodular chromitites (~50 vol. % chromite) are made up of aggregates of anhedral-subhedral, frequently ovoid-like, chromite crystals with grain sizes ranging between 2 and 6 mm (Figure 4b). In the nodular textures, the chromitite nodules are embedded in a serpentinite matrix and exhibit a

well-developed crack-seal filled by chrysotile and opal (Figure 4c). Noteworthy, chromite forming the different chromite textures is unaltered.

3.2. DUNITE AND HARZBURGITE

The dunite envelope around the studied chromitite reaches up to 1.5 m thick and chiefly consists of olivine (up to 0.5 cm) partly transformed to lizardite (Figure 5a to 5d), although some domains with disseminated chromite may contains impregnations (10-15 % modal) of variably bastitized anhedral clinopyroxene (Figure 5e to 5f). Regardless of its pyroxene content dunite contain subhedral grains of accessory chromite (up to 3% modal) and it is crosscut by a well-developed network of late magnesite, chrysotile and opal veins.

Harzburgite displays porphyroclastic texture; it is clinopyroxene-poor and contains ubiquitous crystals (1-2 mm) of subhedral chromite (< 2% modal). Olivine is heavily serpentinized (70%) to a lizardite-magnetite assemblage displaying mesh textures, whereas orthopyroxene and clinopyroxene are pseudomorphed by batiste. The harzburgite also contains accessory crystals of chromite with subhedral and anhedral (*i.e.*, vermicular) morphology, although in lower amounts (< 2% modal) than dunite (Figure 5e to 5f).Similarly to chromite forming the chromitite body, accessory chromite in dunite and harzburgite is unaltered despite of the intense cracking that affected them.
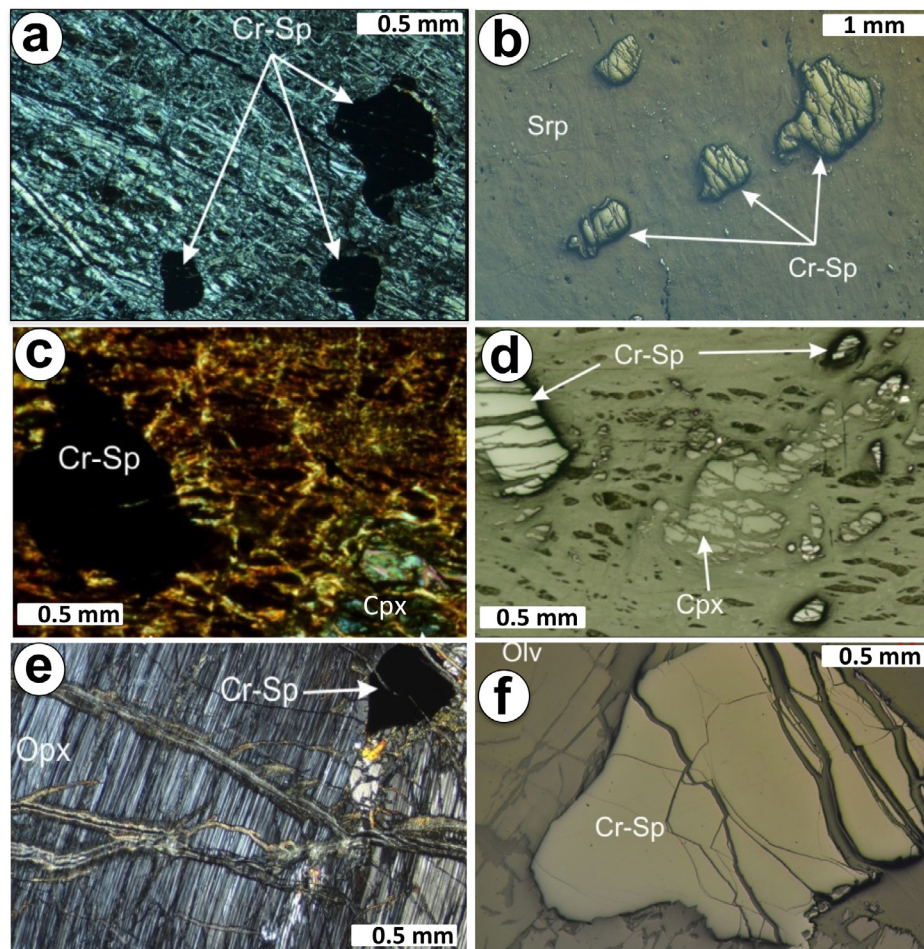
Figure 5 Photomicrographs (transmitted right side and reflected light left side) of chromie in dunite and harzburgite enclosing the Cerro Colorado chromitite. (a–b) irregular chromite in dunite hosting the high-Al chromitite of Cerro Colorado. (c–d) anhedral chromite in clinopyroxene-bearing dunite. (e–f) subhedral chromite in harzburgite. Keys: Cr-sp: chromian spinel; Srp: serpentine.

4. Analytical procedures

4.1. ELECTRON-PROBE MICROANALYSIS

The quantitative analyses of chromite and silicates were obtained by wavelength-dispersive spectrometry (WDS) analysis using a JEOL JXA-8230 at the Centres Científics i Tecnològics of the University of Barcelona (CCiTUB, Barcelona, Spain), operated at 20 kV acceleration voltage, 15 nA beam current and with a beam diameter of 1 µm. Calibration standards were Cr_2O_3 (Cr), corundum (Al), rutile (Ti), periclase (Mg), hematite (Fe), rhodonite (Mn), NiO (Ni), and metallic V. The PAP correction procedure was used for obtaining concentrations (Pouchou and Pichoir, 1985).

4.2. *IN SITU* LASER ABLATION ICPMS

Minor and trace elements in chromite were obtained using *Photon Machines Analyte Excite* 193 nm laser system connected to an Agilent 8800 QQQ ICP-MS in the Instituto Andaluz de Ciencias de la Tierra, Granada, Spain, following the method described in Pagé and Barnes (2009). The chromite analyses were focused on the masses ^{45}Sc, ^{47}Ti, ^{51}V, ^{55}Mn, ^{59}Co, ^{60}Ni, ^{66}Zn and ^{71}Ga, and were conducted using a ~65 µm beam diameter, 10 Hz frequency, and fluence of 10 mJ/cm^2, during 90 s analysis (30 s for the He gas blank and 60 s on the chromite).

The data obtained during ablation runs were processed using the Iolite™ V2.5 program (Paton

Table 2. Ranges of minor and trace elements in chromite from the Cerro Colorado chromitite body and enclosing peridotites. Values are shown in ppm as obtained from LA-ICMPS.

	Massive n = 11		Semimassive n = 12		Dunite n = 11		Harzburgite n = 7	
	Max	Min	Max	Min	Max	Min	Max	Min
^{45}Sc	3.3	2.9	3.78	2.73	6.09	4.16	2.61	1.61
^{47}Ti	1406	1040	1848	1631	1392	1233	413	254.4
^{51}V	1096	1017	1106	1022	1404	1260	1405	1247
^{55}Mn	1162	1096	1148	966	1824	1556	1603	1271
^{59}Co	217.3	205.2	212.9	184.6	365	315.3	488	306.1
^{60}Ni	1178	1008	1138	1042	1726	1369	1068	925
^{64}Zn	434	378	422	377	1229	1006	1707	1073
^{69}Ga	44	41.3	46.7	42.4	41.84	35.8	34.2	31.99

et al., 2011), and aluminum values obtained by electron microprobe were used as the internal standard for chromite. The instrument was calibrated against the NIST 610 silicate glass (National Institute Standards and Technology; Jochum *et al.*, 2011) using Al previously analyzed with EMPA. The basaltic glass BCR-2g (Norman *et al.*, 1996; Gao *et al.*, 2002) and the in-house secondary standard chromite G15-28 (Mercedita, Cuba; Colás *et al.*, 2014) were analyzed as unknowns during each analytical run to check the accuracy and precision of the chromite analyses.

4.3. WHOLE-ROCK ANALYSIS OF PLATINUM-GROUP ELEMENTS

Whole-rock chromitite samples from the studied chromitite body were analyzed for platinum-group elements by at Genalysis Ltd (Perth, Western Australia) using nickel sulfide fire assay collection with ICP-MS (detection limits, 1 ppb for Rh and 2 ppb for Os, Ir, Ru, Pt, and Pd), following the method described by Chan and Finch (2001).

5. Chemistry of chromian spinel and silicates

About 300 single-spot electron-microprobe analyses were carried out on chromite and silicates from polished thin sections from the studied chromitite body as well as from the enclosing dunite and host harzburgite. Additionally, 45 *in-situ* analyses using

LA-ICMP were performed on chromite from chromitite and host peridotites. Representative analysis of chromite and silicates are given in Tables 1 to 3.

5.1. MAJOR AND TRACE ELEMENTS OF CHROMITE IN CHROMITITE, DUNITE AND HARZBURGITE

The chemistry of chromite in the Cerro Colorado chromitite body shows a relatively narrow compositional field (Figure 6a to 6d). The Cr# [(Cr/Cr+Al) atomic ratio] varies from 0.44 to 0.60 (corresponding to 36.3-45.2 Cr_2O_3 and 21-31.2 Al_2O_3) and Mg# [(Mg/Mg+Fe^{2+}) atomic ratio)] from 0.60 to 0.74 (Figure 6a and 6c). There is a trend of increasing of Cr# from the outer part to the core of the body consisting of disseminated (0.44-0.46) and nodular textures (0.44-0.48) to semimassive (0.52-0.54) and massive textures (0.52-0.6) (Figure 6c). The accessory chromite of dunite enclosing this high-Al chromitite has even lower Cr# (0.46-0.59) than chromite of the chromitite and harzburgite (0.52-0.58) (Figure 7). The TiO_2 contents analyzed with EMPA in chromite of the chromitite are relatively higher (up to 0.37 wt.%) than in dunite (0.19-0.31 wt.%) and harzburgite (<0.10 wt.%).

In-situ laser ablation ICP MS analysis was used to determine concentrations of a suite of minor and trace elements (Ti, Ga, Ni, Zn, Co, V and Sc) of chromite from massive chromitites, dunite and harzburgite. To facilitate a comparison of all elements, the data were normalized to the composition of chromite from a mid-ocean ridge basalt

Table 3. Ranges of major and minor elements in silicates from the Cerro Colorado chromitite and enclosing dunite and harzburgite. Values are shown in wt.% as obtained from electron-microprobe.

| | Olivine | | Clinopyroxene | | | | Orthopyroxene | |
| | Chromitite n = 85 | | Cpx-bearing dunite n = 15 | | Harzburgite n = 4 | | Harzburgite n = 11 | |
	Min	Max	Min	Max	Min	Max	Min	Max
SiO_2	39.95	41.27	50.69	52.45	51.65	52.4	54.44	55.51
TiO_2	0	0.06	0.16	0.24	0	0.09	0	0.02
Al_2O_3	0	0.39	2.73	4.24	2.82	3.14	2.14	2.56
V_2O_3	0	0.05	0	0.07	0.01	0.07	0	0.04
Cr_2O_3	0	0.07	0.79	1.21	1.32	1.53	0.67	0.96
Fe_2O_3t	5.9	7.2	2.15	2.55	2.41	2.5	5.62	6.09
MgO	51.23	53.1	15.58	16.7	16.48	16.81	32.2	34.33
CaO	0.02	0.07	24.06	24.67	23	23.26	0.8	3.68
MnO	0.07	0.14	0.01	0.08	0.08	0.11	0.14	0.17
NiO	0.39	0.52	0.02	0.09	0.05	0.09	0.08	0.12
Na_2O	0	0.04	0.35	0.54	0.59	0.68	0.02	0.15
K_2O	0	0.01	0	0.01	0	0.01	0	0.01
Mg#	0.93	0.94	0.93	0.92	0.92	0.92	0.91	0.91

(MORB) (Figure 8a to 8b), and plotted in order of compatibility in chromite (Pagé and Barnes, 2009; González-Jiménez *et al.*, 2017b). Chromite forming massive chromitite has levels of Ti (1040-1848 ppm), Ga (41-47 ppm), Zn (377-434 ppm), Co (185-217 ppm) and Mn (966-1162 ppm) similar to chromite from MORB, but slightly higher V (1017-1106 ppm) and lower Sc (< 4 ppm) and Ni (1008-1178 ppm) (Figure 8a; Table 2). Accessory chromite in the dunite also has Ti (1233-1392 ppm) and Ni (1369-1726 ppm) similar to MORB but higher V (1260-1404 ppm), Zn (1006-1229 ppm), Co (315-365 ppm) and Mn (1556-1824 ppm) and slightly lower Sc (4-6 ppm), Ga (36-42 ppm) and Ni (1369-1726 ppm) (Figure 8b; Table 2. Chromite in harzburgite has even higher content of V (1247-1405 ppm), Zn (1073-1707 ppm), Co (306-488 ppm) and Mn (1271-1603 ppm) but much lower of Sc (2-3 ppm), Ga (32-34 ppm), Ti (254-413 ppm) and Ni (925-1068 ppm) than chromite in chromitite, dunite and MORB reference (Figure 8b; Table 2).

5.2. SILICATES IN CHROMITITE, DUNITE AND HARZBURGITE

Unaltered olivine useable for electron-microprobe analyses has only been preserved in the matrix of massive chromitite. These olivines are forsterite (Mg# = 0.93), containing NiO (0.43 wt.%) and MnO (0.11 wt.%) (Table 3).

Clinopyroxene in dunite has relatively high Mg# (0.92-0.93) which roughly correlates inversely with Cr_2O_3 (0.79-1.21 wt.%) and Al_2O_3 (2.73-4.24 wt%); the TiO_2 content reaches 0.24 wt.% and Na_2O is lower than 0.54 wt.% (Figure 9a to 9c; Table 3). Clinopyroxene in harzburgite exhibits similar high Mg# (0.92), although with higher Cr_2O_3 (1.32-1.53 wt.%) and overall lower Al_2O_3 (2.82-3.14 wt.%) and TiO_2 (<0.09 wt.%) (Figure 9a to 9c; Table 3).

Orthopyroxene in harzburgite enclosing the pair chromitite-dunite has slightly lower Mg# (0.91), Cr_2O_3 (0.66-0.96 wt.%), Al_2O_3 (2.14-2.56 wt.%) and TiO_2 (<0.02 wt%) and Al_2O_3 than clinopyroxene (Figure 9e to 9f; Table 3).

6. Bulk-rock geochemistry of platinum group elements

The total PGE abundances in the studied chromitite body range between 60 and 109 ppb (average: 93 ppb), having the nodular chromitites samples lower values (60 ppb) than massive ones (96-109
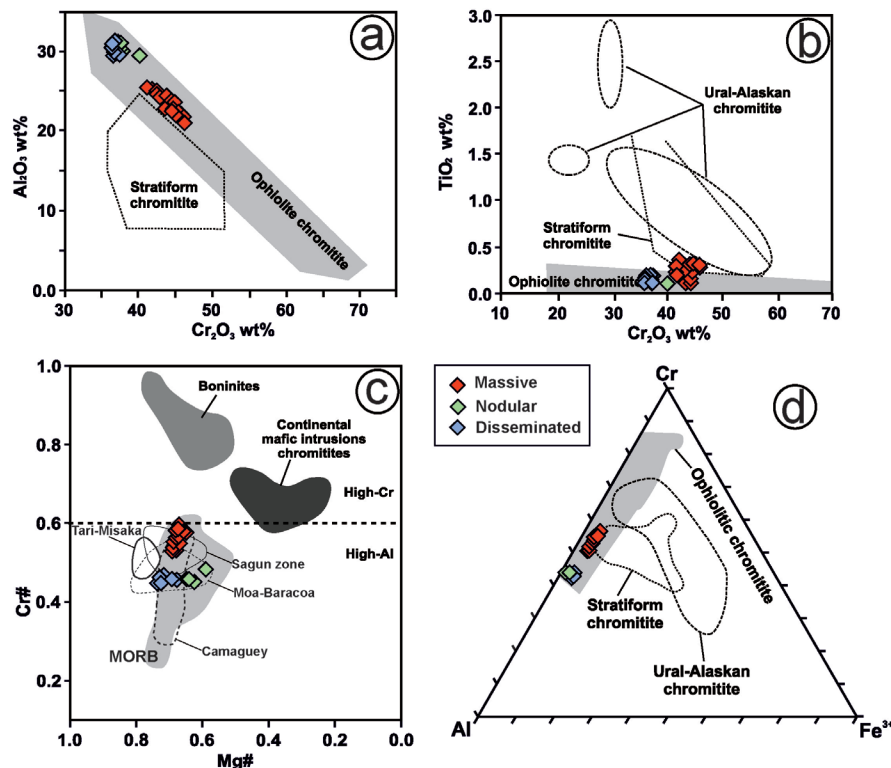
Figure 6 Chemistry of primary chromites from the Cerro Colorado chromitite as compared to chromite from various tectonic settings in terms of (a) Al_2O_3 vs. Cr_2O_3, (b) TiO_2 vs Cr_2O_3, (c) Cr# [Cr/(Cr+Al) atomic ratio] vs Mg# [Mg/(Mg+Fe) atomic ratio] and (d) Al-Cr-Fe^{3+} compositions. Data sources for chromian spinel of different tectonic settings are Bonavia *et al.* (1993), Kamenetsky *et al.* (2001) and Proenza *et al.* (2007). Legend is inset in the figure (note that semi-massive samples shown in Table 1 include also the nodular chromitite plotted in the figure).

ppb) (Figure 10; Table 4). The gold contents vary between 2 and 13 ppb. Overall, the analyzed samples have almost identical total contents of IPGE (Os+Ir+Ru=38-56 ppb; average: 39 ppb) and PPGE (Pt+Pd+Rh=65-16 ppb; average: 35). This distribution of the PGEs produces relatively flat PGE-chondrite normalized patterns, although nodular chromitites exhibit remarkable negative anomalies in Os, Pt and Pd (Figure 10).

7. Discussion

7.1. PARENTAL MELTS OF THE CHROMITITE

Chromite of the Cerro Colorado chromitite displays relatively high Al_2O_3 (21-31.2 wt.%) and low Fe_2O_3 (<4.5 wt.%) and TiO_2 (< 0.37 wt.%) contents (Figura 6a, 6b and 6d; Table 1). This composition is typical of the chromite forming the high-Al chromitites that are usually found hosted in the mantle section of ophiolite complexes (Figure 6a to 6d), overlapping — at least in terms of major elements— that of chromian spinel from MORB sources (Figure 11a to 11d). Nevertheless, the slight differences in the chemistry of chromite forming massive, disseminated and nodular chromitite (Figure 6a and 6d) may reflect significant element exchange (mainly Fe^{2+} and Mg) between chromite and host peridotites during subsolidus re-equilibrium upon cooling of the chromitite body (Bussolesi *et al.*, 2019 and references therein). Therefore, only composition of massive samples (*i.e.*, nearly monomineralic chromite) should be used to estimate the nature of the parental melts. Several experimental (Maurel and Maurel, 1982; Wasylenki *et al.*, 2003) and empirical works (*e.g.*, Kamenetsky *et al.*, 2001) have shown that Al_2O_3,

TiO$_2$ contents and FeO/MgO in chromites is a direct function of the contents of Al$_2$O$_3$, TiO$_2$, FeO and MgO in the melt from which chromite had crystallized. A comparison of the geochemistry of chromite forming chromitites hosted in mantle rocks and associated extruded lavas has validated the feasibility of this approach showing that there is a link between the composition of the melt and chemistry of chromite (*e.g.*, Rollinson, 2008; Pagé and Barnes, 2009; Farahat *et al.*, 2011). Thus, the Al$_2$O$_3$ content in the melt can be estimated from the Al$_2$O$_3$ content from chromite using the equation proposed by Maurel and Maurel (1982):

$$(Al_2O_3)_{chromite} = 0.035(Al_2O_3)^{2.42} \qquad [1]$$

or alternatively/complementary by using the empirical power-law expression proposed by Rollinson (2008) for MORB melts, which was partially derived from Kamenetsky *et al.* (2001):

$$(Al_2O_3)_{melt} = 4.13686 \ Ln \ (Al_2O_3)_{chromite} + 2.2828 \ (R^2 = 0.6649) \qquad [2]$$

The application of these two formulations to massive chromitites forming chromitites in different geotectonic settings (*e.g*, continental and oceanic lithosphere) have shown that the Al$_2$O$_3$ contents of the melt in equilibrium with chromite estimated by both methods correspond closely (*e.g*, Uysal *et al.*, 2009; González-Jiménez *et al.*, 2011a; Mukherjee *et al.*, 2010; González-Jiménez *et al.*, 2017b). Additionally, the TiO$_2$ content in the melt from which the high-Al chromite of Cerro Colorado crystallized can be also extracted using the TiO$_2$ content measured in the high-Al chromite by applying the empirical equation obtained by Kamenetsky *et al.* (2001) for chromite of MORB sources:

$$(TiO_2)_{melt} = 0.708 \ Ln \ (TiO_2)_{chromite} + 1.6436 \ (R^2 = 0.8455) \qquad [3]$$

while the FeO/MgO ratio of the melt can also be computed using the formula proposed by Maurel and Maurel (1982):
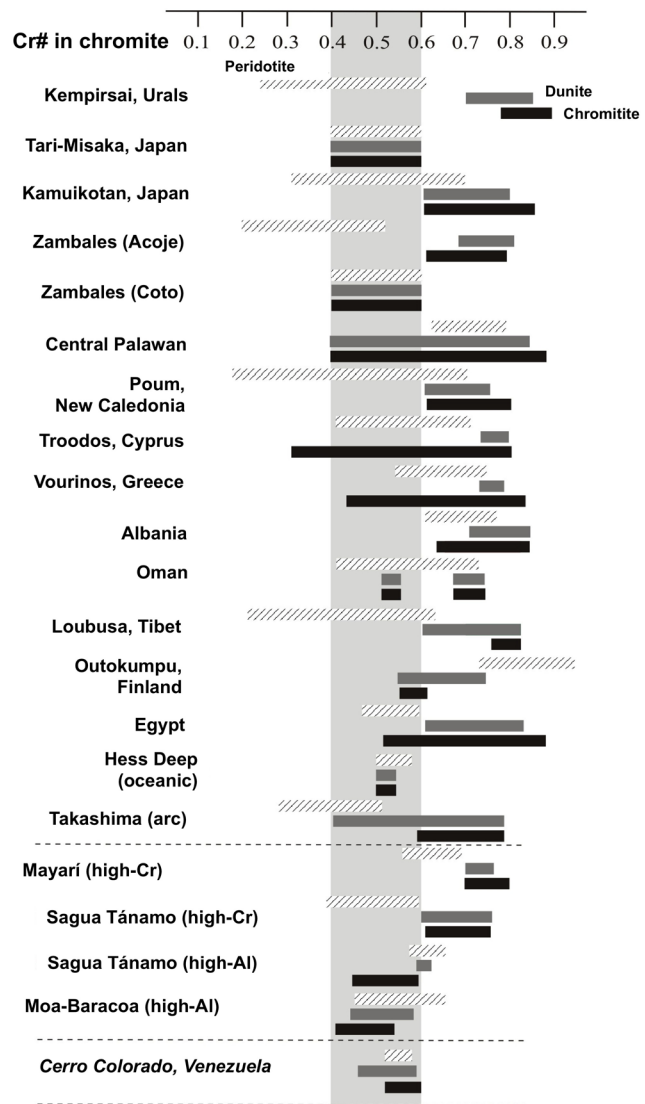

Figure 7 Comparison of Cr# in chromite from chromitites and enclosing host rocks of Cerro Colorado, and in podiform high-Cr and high-Al chromitites of some ophiolitic complexes. Data sources for high-Cr chromitites: CED, Egypt (Ahmed *et al.*, 2001); Kempirsai, Kazakhastan (Melcher *et al.*, 1994, 1997, 1999); S. Kamuikotan, Japan (Arai, 1997); Acoje, Philippines (Rammlmair *et al.*, 1987); Troodos, Cyprus (Augé and Johan, 1988; McElduff and Stumpfl, 1991); Vourinos, Greece, (Economou, 1983; Economou *et al.*, 1986; Economou-Eliopoulos, 1996); N. Oman (Ahmed and Arai, 2002; Rollinson, 2005); Albania (Kocks *et al.*, 2007); Poum, New Caledonia (Leblanc, 1995); Luobusa, China (Zhou and Bai, 1992; Zhou and Robinson, 1994; Peng *et al.*, 1995; Zhou *et al.*, 1996); Mayarí and Sagua de Tánamo in Cuba (Proenza *et al.*, 1999; Gervilla *et al.*, 2005; González-Jiménez *et al.*, 2011a). Data sources for high-Al chromitites: CED, Egypt, Outokumpu, Finland, and Tari-Misaka, Japan (Arai, 1997 in Ahmed *et al.*, 2001); Sartohay, China (Zhou and Bai, 1992; Zhou and Robinson, 1994; Peng *et al.*, 1995; Zhou *et al.*, 1996); Moa-Baracoa, Cuba (Proenza *et al.*, 1999; Gervilla *et al.*, 2005).
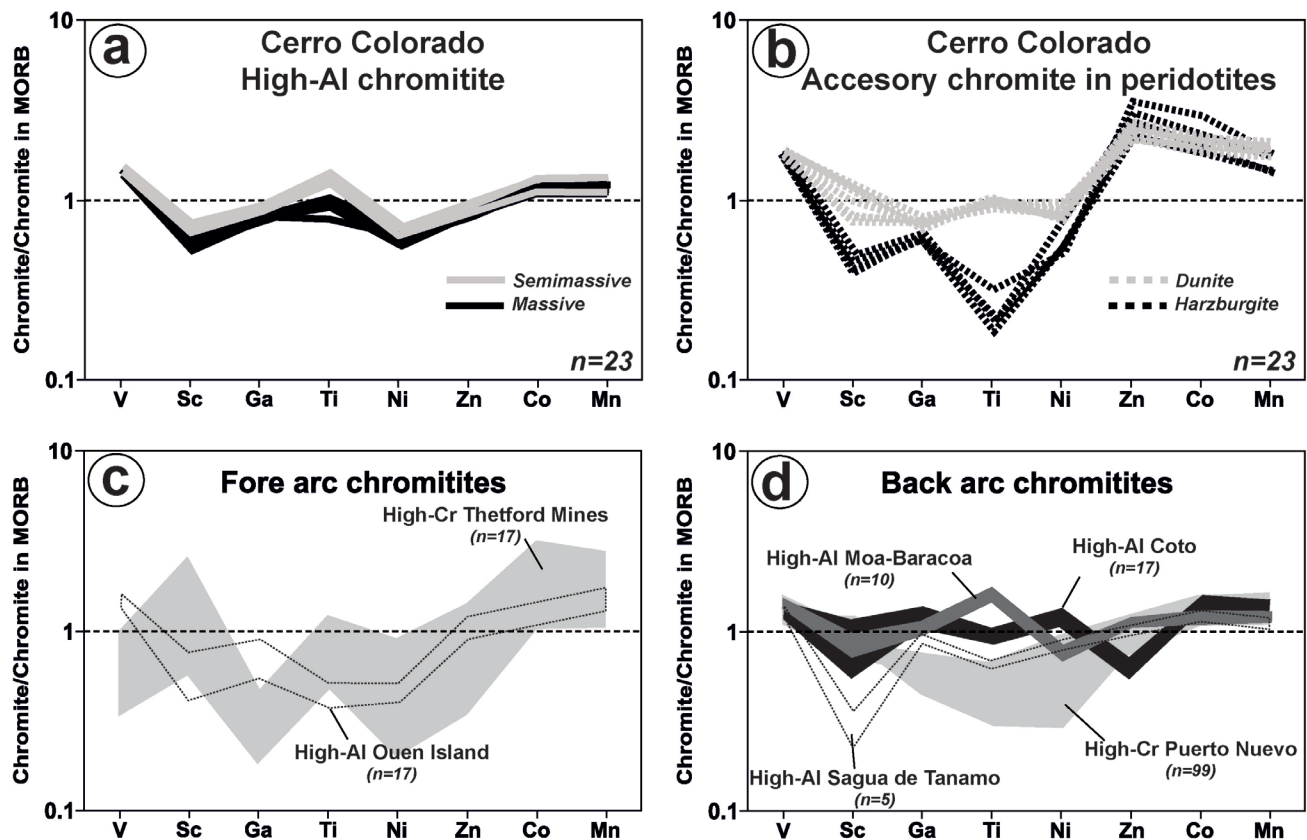
Figure 8 Spider diagrams showing the composition of minor and trace elements of chromite of massive and semimassive chromitite of the Cerro Colorado chromitite body and enclosing dunite and harzburgite (a-b) and comparison with other representative low-pressure chromitites from fore-arc and back-arc regions of supra-subduction zone ophiolites (c-d). Data sources for chromitites from the fore-arc mantle are Thetford Mines (Pagé and Barnes, 2009), Ouen Island in New Caledonia (González-Jiménez *et al.*, 2011b) whereas those from back-arc mantle are from the eastern Cuban mining districts of Sagua de Tánamo (González-Jiménez *et al.*, 2015) and Moa-Baracoa (Colás *et al.*, 2014), the Mexican ophiolite of Puerto Nuevo (González-Jiménez *et al.*, 2017b) and Coto in Philippines (Yao, 1999).

$$\mathrm{Ln(FeO/MgO)_{chromite}} = 0.47 - 1.07\mathrm{Al\#_{chromite}} + 0.64\mathrm{Fe^{3+}\#chromite} + \mathrm{Ln(FeO/MgO)_{melt}} \quad [4]$$

with FeO and MgO in wt.%, Al#=Al/(Cr+Al+Fe^{3+}) and Fe^{3+}#=Fe^{3+}/(Cr+Al+Fe^{3+}).

The estimated melt compositions in equilibrium with the Cerro Colorado high-Al massive chromitites of the main body have 14.88-15.7 wt.% Al$_2$O$_3$ and highly variable TiO$_2$ (0.5-0.9 wt.%; average 0.72 wt%) and FeO/MgO ratios (0.95-1.13) (Figure 11a to 11d; Table 5). These results suggest that the Cerro Colorado high-Al chromitite body crystallized from melts with composition broadly similar to MORB in terms of Al$_2$O$_3$ (15-16 wt.%). However, the obtained TiO$_2$ and FeO/MgO are overall lower than in MORB

melts, suggesting an affinity closer to back-arc basin basalts (*e.g.*, Dick and Bullen, 1984; Willson, 1989; Mudholkar and Paropkari, 1999). High-Al cromitites that have crystallized from melts with identical Al$_2$O$_3$ contents to those that formed the chromitite body studied here are known from other Mesozoic ophiolites of the Great Antilles Arc (Moa-Baracoa and Sagua de Tánamo mining districts in eastern Cuba; Proenza *et al.*, 1999; González-Jiménez *et al.*, 2011a) as well as in Muğla and Elekdağ in Turkey (Uysal *et al.*, 2009; Dönmez *et al.*, 2014) and Oman (Rollinson, 2008) (Table 5). Similarly to observations in this study, all these high-Al chromitite were found located in the shallowest portion of the upper mantle section of the oceanic lithosphere, within the mantle-crust transition zone (*i.e.*, Moho Transition Zone or

Table 4. Concentration (ppb) of platinum-group elements in the Cerro Colorado chromitite.

Sample	Type	Os	Ir	Ru	Rh	Pt	Pd	Total	IPGE	PPGE	Pd/Ir
PP3	Nodular	10	12	22	3	10	3	60	44	16	0.3
PP5C	Massive	4	17	23	4	24	37	109	44	65	2.2
PP5D1	Massive	11	18	26	4	22	15	96	55	41	0.8
PP10B	Massive	7	19	26	3	23	27	105	52	53	1.4

MTZ) of the ophiolite. All these chromitites were interpreted to have precipitated from N-MORB or BABB melts in the shallow upper mantle, within the MTZ of oceanic lithosphere originated or modified in a SSZ back-arc setting.

7.2. TRACE ELEMENT FINGERPRINTS IN CHROMITITE FOR THE TECTONIC SETTING OF FORMATION

Valuable information on the geochemical signature of the parental magmas and the tectonic setting of their genesis can be also obtained by studying the distribution of a suite of minor and trace elements in chromite (including V, Sc, Ga, Ti, Ni, Zn, Co and Mn) and platinum-group elements (Os, Ir, Ru, Rh, Pt and Pd) in the chromitite. A comparison of the MORB-normalized patterns of the chromitites analyzed in this study with other chromite from well constrained tectonic settings (Figure 8) reveals that they are clearly distinct to those displayed by igneous chromite forming the high-Cr chromitites found in the back-arc (*e.g.*, Sagua de Tánamo in Cuba) or fore-arc (*e.g.*, Thetford Mines in Canada) (Figure 8c) mantle sections from some ophiolites, whose chromite spidergrams have more affinity with those chromite from fore-arc boninites (Figure 8c). Rather the chromitites studied here are akin to those hosted in the back-arc mantle of the Cuban and Philippine ophiolites (Figure 8d). It is worth to note that Cerro Colorado chromitite exhibit MORB-normalized patterns strongly similar to that reported for chromitites of the Mercedita chromite deposit in the Mayarí-Baracoa ophiolitic belt in Cuba. The Mercedita chromitite is also hosted in a mantle with frequent gabbro sills and dikes, which has been interpreted as the petrological Moho Transition Zone of an oceanic

lithosphere originated in the rear of the Cretaceous Great Antilles island arc (Proenza *et al.*, 1999; Gervilla *et al.*, 2005; Pujol-Solà *et al.*, 2018).

Empirical and experimental estimations (*e.g.*, Bockrath *et al.*, 2004; Prichard *et al.*, 2008; Fonseca *et al.*, 2012, 2017; Luguet and Reisberg, 2016) have shown that appreciable concentration of the PGE > 100 ppb can only occur in mantle melts that have been from relatively depleted mantle source after relatively high rates of partial melting, at about 20%. The fact that in the Cerro Colorado chromitite the total PGE content is overall less than ~100 ppb (< 109 ppb; Table 4) suggest that partial melting degrees were not far beyond 20%. These rates of partial melting are typically produced in fast-spreading centers in mid-ocean ridges or relatively mature back-arc basins originated in the rear of intra-oceanic island arcs.

In the latter settings, melting of fertile or moderately depleted peridotite takes place in relatively anhydrous conditions, which are not enough to remove PGE-bearing minerals such as sulfides and alloys and release PGE into the produced silicate melt (*e.g.*, Prichard *et al.*, 2008; Luguet and Reisberg, 2016). These types of melts are usually S-saturated and therefore partition all the PGE almost equally, therefore chromitites crystallized from them are characterized by PGE-normalized patterns with no significant fractionation between IPGE (Os, Ir, Ru) and PPGE (Pt, Pd, Rh) such as observed in the Cerro Colorado chromitite.

These clearly contrast with the typical negative-slope (*i.e.*, enrichment in Os-Ir-Ru over Pt-Pd-Rh) of the PGE-patterns that usually display mantle chromitite originated in the fore-arc or back-arc mantle in supra-subduction zones (*e.g.*, González-Jiménez *et al.*, 2014), whose parental melts are usually extracted from relatively depleted
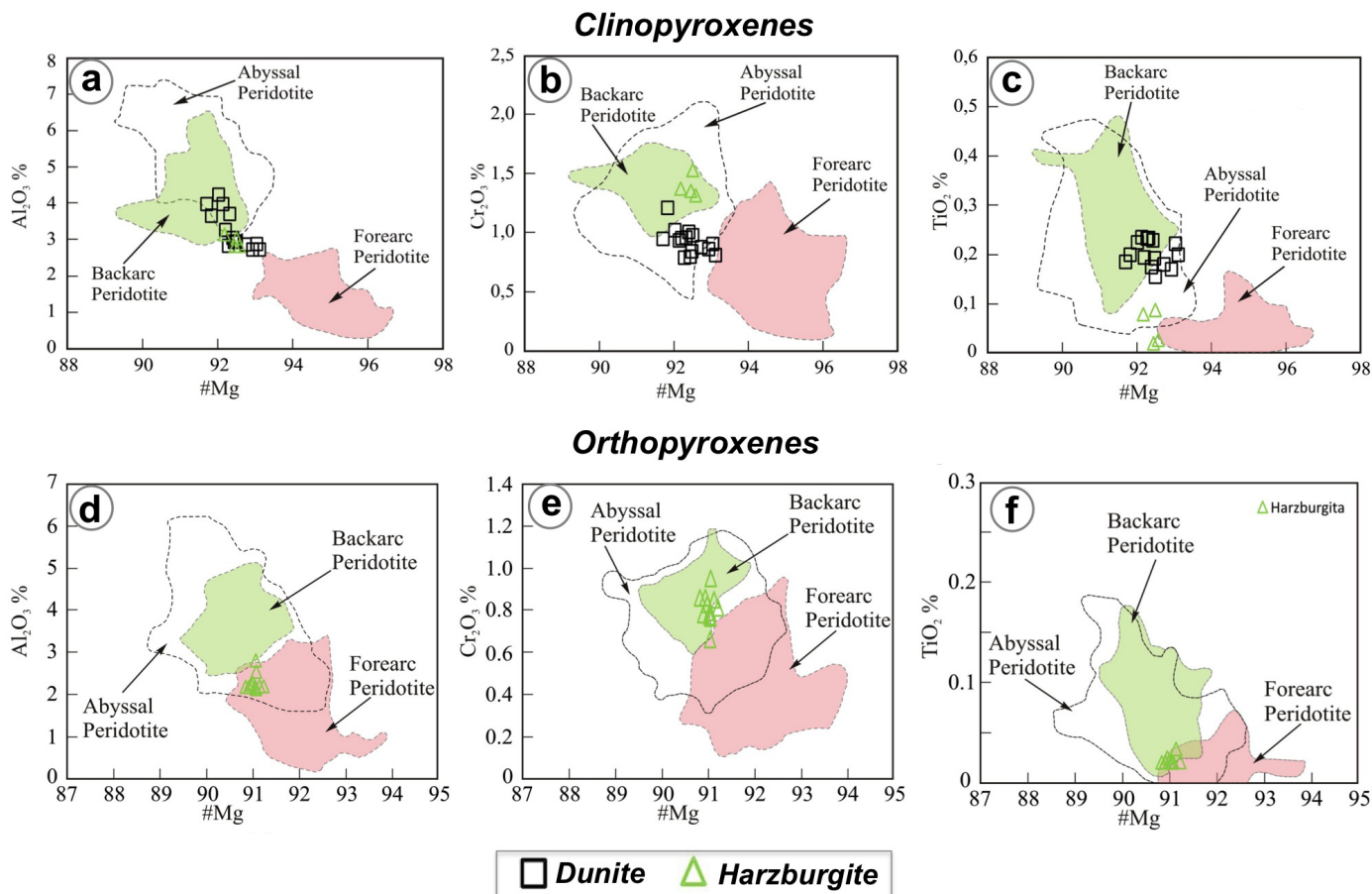
Clinopyroxenes

Orthopyroxenes

☐ *Dunite*   △ *Harzburgite*

Figure 9 Compositional variations of pyroxenes in dunite and harzburgite enclosing the high-Al chromitite of Cerro Colorado.

or moderately depleted sub-arc peridotites that have experienced higher rates of hydrous partial melting aided by the infiltration of slab-derived fluids.

On the other hand, some of the chromitite samples analyzed from the studied chromitite body display relative enrichment in Pd and Au (Figure 10; Table 4). This is a relatively unusual characteristic of mantle-hosted chromitite, which is usually attributed to post-magmatic remobilization of these metals. Secondary enrichment in Pd and gold is a distinctive feature of chromitites altered by hydrothermal fluids related with serpentinization and/or metamorphism (Thalhammer *et al.*, 1990; Tarkian *et al.*, 1991; Yang and Seccombe, 1993; Graham *et al.*, 1996; Malitch *et al.*, 2001; Proenza *et al.*, 2008; González-Jiménez *et al.*, 2016). Of particular interest is the silica-carbonate (litsvenitization) alteration that has precipitated magnesite and opal in the secondary crack-seal of

the Cerro Colorado chromitite (Martín-Belliza, 1960; Franco and Torrealba, 1987; Mistage *et al.*, 1989). Several studies have shown that this style of post-magmatic alteration is a very effective in the remobilization and concentration of gold (of up to 1000 times the original value) in ultramafic rocks and associated chromitites (Buisson and Leblanc, 1986; Escayola *et al.*, 2009; Buckman and Ashley, 2010; Azer, 2013).

Summarizing, the Cerro Colorado chromitite has geochemical fingerprints for chromite and bulk-rock PGE that are compatible with those chromitites hosted in the oceanic mantle (back-arc mantle) section of SSZ ophiolites. This is consistent with the fact that the chromitites associated with gabbro sills with no evidence of HP/UHP metamorphism, similarly the ordinary low-pressure high-Al chromitites reported from the Moa-Baracoa ophiolitic massif in eastern Cuba (*e.g*, Pujol-Solà *et al.*, 2018).

Table 5. Calculation of Al_2O_3 and TiO_2 contents and FeO/MgO ratios of the melts in equilibrium with chromite from the Cerro Colorado chromitite and other high-Al chromitites from Mesozoic ophiolites. The values for boninites and MORB are also presented for comparison. Ti values in the melt have been computed using the values obtained from the electron-microprobe analysis.

	Al_2O_3 liquid (wt%)	TiO_2 liquid (wt%)	FeO/MgO liquid (wt%)
Cero Colorado	14.8-15.7	0.5-0.9	0.9-1.3
Sagua de Tánamo [a]	15-16	0.3-0.5	0.9-1.1
Moa-Baracoa [a]	16.4	0.9	0.9
Elekdağ[b]	14.7-17.3	0.5-1	0.3.08
Muğla [c]	15.2-15.9		0.7-1.1
Oman [d]	14.5-15.4	0.4-0.9	
Boninitite [e]	10.6-14.4	0.1-0.5	0.7-1.4
MORB [f]	15-16		1.2-1.6

[a] **Proenza *et al.* (1999) and González-Jiménez *et al.* (2011a, 2011b),** [b] **Dönmaz *et al.* (2014),** [c] **Uysal *et al.* (2009),** [d] **Rollinson (2008),** [e] **Hicky and Frey (1982), and** [f] **Wilson (1989).**

7.3. FORMATION OF THE CERRO COLORADO CHROMITITE BODY

As noted above, in the high-Al chromitite of Cerro Colorado the relations between Al_2O_3 and TiO_2 shows that the composition of chromite in chromitite overlaps the fields of MORB and spinel from modern back-arc basin basalts (Figure 11c). Similarly, the compositions of accessory chromite found in the host dunite envelope and harzburgite also span over the overlapping field of MORB and spinel from back-arc basin basalts (Figure 8b to 8d). This suggests a back-arc affinity, consistent with the composition of the melt estimated in equilibrium with chromite of the chromitite, distribution of trace element in chromite and bulk-rock PGE. Moreover, in plots Cr# vs. Mg# the chemistry of clinopyroxene and orthopyroxene found in the country peridotite overlap the fields of abyssal (MORB) and back-arc (Figure 11c), whereas coexisting gabbro and basalts have also back-arc affinity (Santamaría and Schubert, 1974, Baquero *et al.*, 2013). Interestingly, chromite from chromitite and dunite exhibit almost identical Cr contents, which are broadly similar and higher respectively than chromite from host harzburgite (Figure 7). This observation indicates that chromitite and dunite very likely crystallized in equilibrium from a common parental melt that was slightly different from those extracted during the formation of the harzburgite. Indeed

the formation of the chromitite-dunite pair involved the reaction of mantle harzburgite with a melt slightly richer in Al and Ti (BABB) than the one involved in the formation of accessory chromite (MORB affinity) in harzburgite. In the chromitites, the higher Cr# and TiO_2 in massive samples compared with nodular and disseminated samples may reflect the fact that migrating melts with BABB affinity have had their composition by the reaction with the country harzburgite. Thus, during melt-rock processes under increasing melt/rock ratio the primitive BABB-like melt became progressively enriched in silica content and Cr#, thus explaining the observed chemical trend in chromite from country harzburgite to the chromitite-dunite pair (Figures 7 and 8; Zhou *et al.*, 1994; Morishita *et al.*, 2011; González-Jiménez *et al.*, 2011a). These chemical trends in the major elements were also accompanied by increasing of Sc, Ga and Ni but decreasing Zn, Co Mn from country harzburgite to the chromitite-dunite pair (Figure 8a and 8b). It has been shown by empirical (Pagé and Barnes, 2009, Dare *et al.*, 2009) and experimental studies (Mallmann, *et al.*, 2009) that Sc and Ga contents correlate positively with f O_2 in chromian spinel. This leads us to suggest that the selective enrichment of incompatible elements shown by chromian spinel of the Cerro Colorado chromitites was associated with a progressively increasing of f O_2 in the parental melt(s). This situation is typical in the back-arc mantle wedge
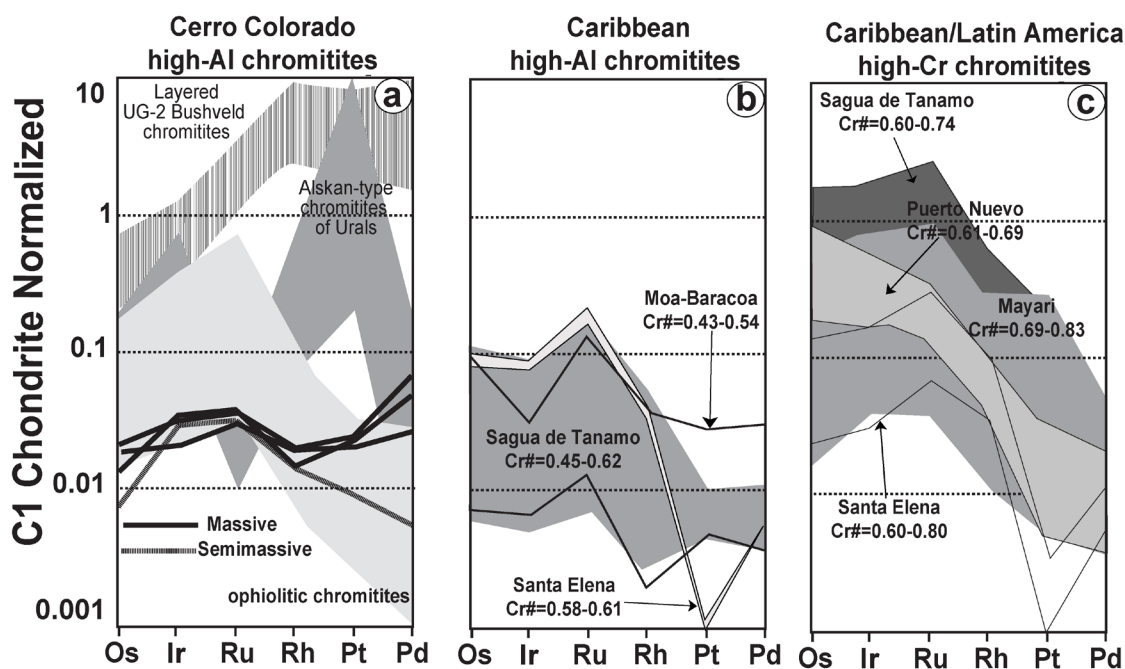
Figure 10 C1-chondrite (Naldrett and Duke, 1980) normalized patterns of the Cerro Colorado chromitite and comparison with chromitites from different crustal settings and hosted in the mantle section of ophiolites. (a) chromitites in Ural-Alaskan-type complexes (Garuti *et al.*, 2005) of the Urals and the Bushveld (UG2) Layered Complex (Naldrett *et al.*, 2012) and ophiolites (Proenza *et al.*, 2007). (b) Caribbean high-Al chromitites (Sagua Tánamo and Moa-Baracoa in Cuba; Gervilla *et al.*, 2005; González-Jiménez *et al.*, 2011a), Santa Elena in Costa Rica (Zaccarini *et al.*, 2011). (c) Caribbean and other Latin American high-Cr chromitites including Sagua Tánamo and Moa-Baracoa in Cuba (Gervilla *et al.*, 2005; González-Jiménez *et al.*, 2011a), Santa Elena in Costa Rica (Zaccarini *et al.*, 2011) and Puerto Nuevo in Mexico (González-Jiménez *et al.*, 2017b).

of suprasubduction zones, where relatively more oxidized melts can form compared with typical MORB (Parkinson and Arculus, 1999) In this scenario, the crystallization of the chromitite would account by hybridization as a result of mixing/mingling of different batches of BABB melt within the dunite conduit continuously replenished by hotter primitive melts. The disseminated and nodular chromitite would record different steps of the progression of the primitive melt infiltration that have promoted melt-rock reaction, dunite formation and melt mixing/mingling within the dunite channel (González-Jiménez *et al.*, 2014).

7.4. GEODYNAMIC AND METALLOGENIC IMPLICATIONS

The structure of the present margin of the northern part of South America in Venezuela is the result of accretion of several convergent-basin complexes between the Jurassic-Cretaceous. The geology and tectonic evolution of the Caribbean plate indicate that during Lower Cretaceous multiple spreading centers were developed in the realm (hanging wall) of the intra-oceanic Great Antilles Arc (Pindell *et al.*, 2012). Remnants of these back-arc basins (LREE-depleted MORB) are now preserved in ophiolites exposed in the continental crust of Venezuela, Costa Rica and Guatemala, and in the mainland of the islands of Cuba and La Hispaniola (Giunta *et al.*, 2002). Many of these ophiolites contain chromitites with compositions varying between high-Cr and high-Al, which have been related with the existence of melts that originated in different magmatic sources of the ophiolite environment (*i.e.*, MOR, SSZ and arc regions) at different times during the formation and/or evolution of this oceanic lithosphere (*e.g.*, Proenza *et al.*, 1999; Lewis *et al.*, 2006; Gervilla *et al.*, 2005;
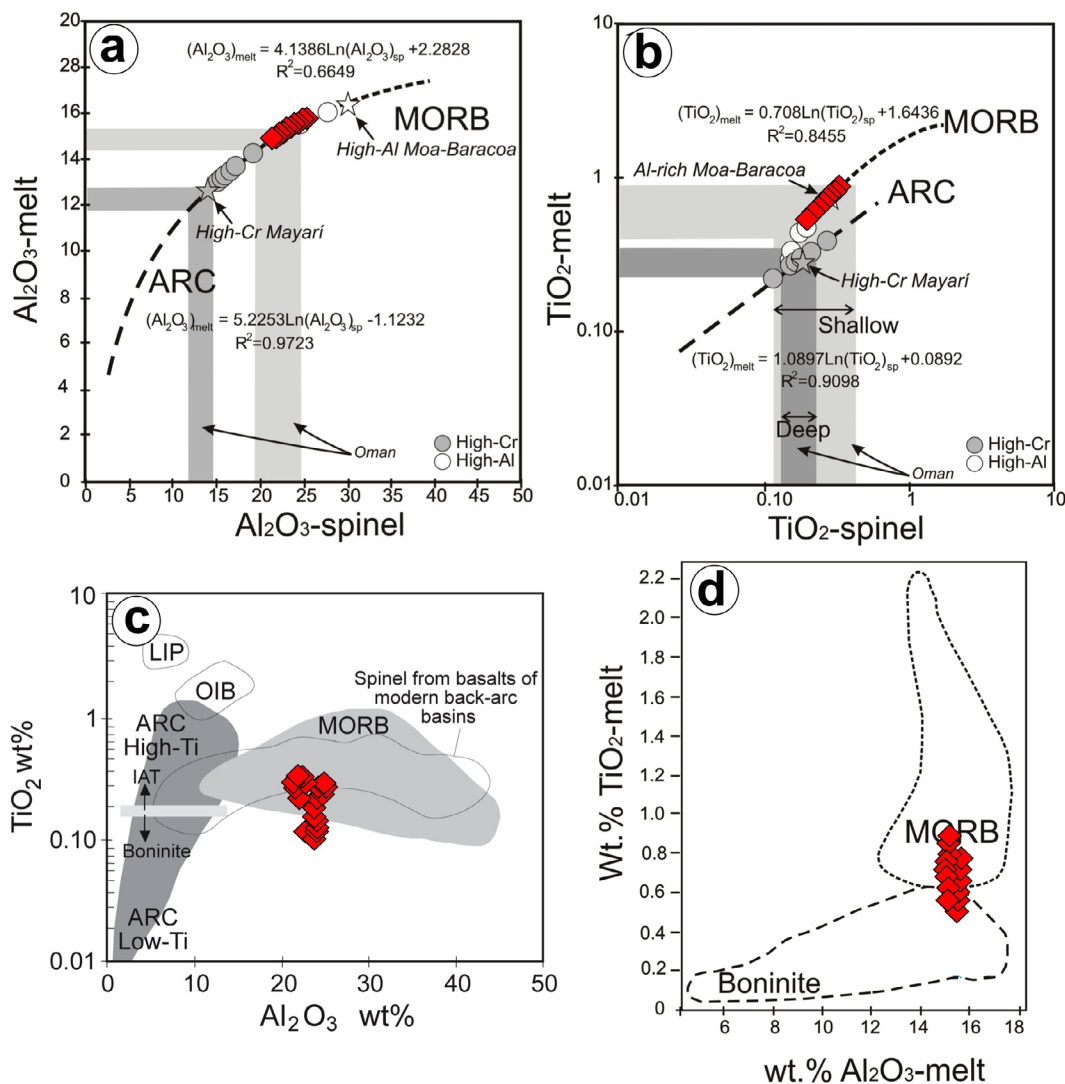
Figure 11 Al_2O_3 (a) and TiO_2 (b) contents of the melt in equilibrium with the Cerro Colorado high-Al chromite. The regression lines are from Zaccarini *et al.* (2011) using data on chromite-melt inclusions in MORB and arc lavas reported by Kamenetsky *et al.* (2001) and Rollinson (2008). The range of chromite and the calculated melt compositions from the shallow and deep Wadi Rajmi chromitites in Oman (Rollinson, 2008), and for high-Al and high-Cr chromitites from Mayarí-Baracoa ophiolitic belt in eastern Cuba (González-Jiménez *et al.*, 2011a) are shown for comparison. Only data of massive chromitite samples were used for computation. (c) Chemistry of chromite of massive chromitites forming the Cerro Colorado chromitite plot in terms of TiO_2 versus Al_2O_3. Data sources for chromian spinel of different tectonic settings were obtained after Kamenetsky *et al.* (2001) and from the compilation of plots shown in Proenza *et al.* (2007). (d) TiO_2 and Al_2O_3 (wt. %) content of the melt calculated to be in equilibrium with chromite from the Cerro Colorado chromitite compared to the fields for chromites from boninites and MORB sources (after Pagé and Barnes, 2009).

González-Jiménez *et al.*, 2011a; Marchesi *et al.*, 2011). For example, the formation of the high-Al chromitites of the Moa-Baracoa ophiolite in eastern Cuba has been associated with tholeiitic magmas (BABB) originated in a relatively evolved back-arc basin (Proenza *et al.*, 1999; Gervilla *et al.*, 2005). The formation and evolution of this ophiolite is dated between 90-125 Ma (Iturralde-Vinent

et al., 2006; Rojas-Agramonte *et al.*, 2016) and igneous zircons recovered from these high-Al chromitite yield ages of 99-118 Ma that overlap, within uncertainty, the U-Pb age of zircons from a Fe-Ti-rich gabbro intruding the mantle peridotite section at the Moa-Baracoa ophiolitic massif (124 ± 1Ma; Rojas-Agramonte *et al.*, 2016). Interestingly, K-Ar ages obtained for basalts and gabbros
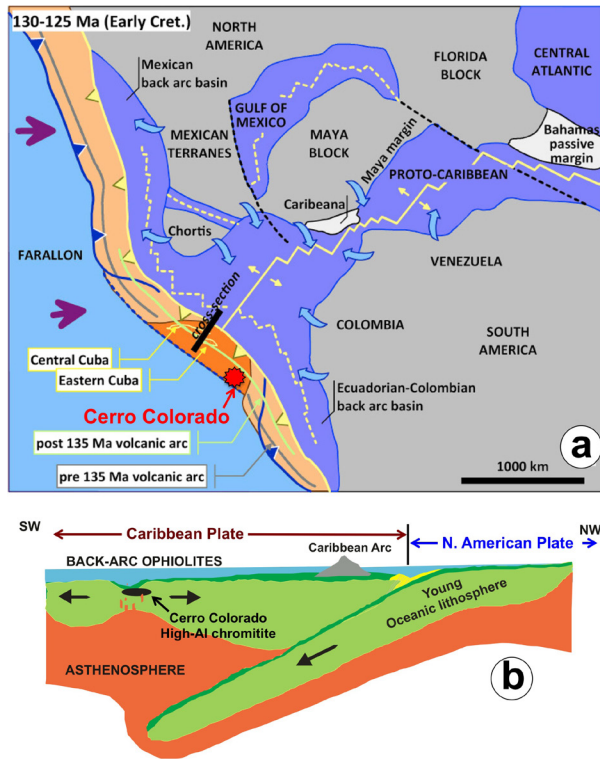
Figure 12 **(a) Paleogeography and tectonic reconstruction of the Caribbean region (modified from Proenza *et al.*, 2018 and references therein) showing the Lower Cretaceous onset of subduction of the Proto-Caribbean lithosphere with reference to the paleogeographical location of the Cerro Colorado and equivalent Cuban ophiolites. (b) Cross-section drawing showing the tectonic setting of formation of the Cerro Colorado high-Al chromitite in the rear of the Caribbean arc (i.e., Greater Antilles arc) during Lower Cretaceous.**

of the oceanic crust of Cerro Colorado ophiolite overlap that of the Moa-Barcoa ophiolite (118-129 Ma; Santamaría and Schubert, 1974) while U-Pb dating of zircons from these gabbros yield 121.7 ± 2 Ma (Baquero *et al.*, 2013). Assuming that at Cerro Colorado the chromitites formed co-genetically with the crustal gabbros, the scenario above suggest that the high-Al chromitites of Cerro Colorado may have formed synchronically and in an analogous tectonic setting than high-Al chromitites from eastern Cuban ophiolites (Figure 12).

On the other hand, the podiform-like chromitite body in the Cerro Colorado ophiolite with Cr_2O_3= 35-45 wt.%, low Fe contents (Cr/Fe= 2.6), Al_2O_3 >20 wt.% and $Cr_2O_3 + Al_2O_3$> 60 wt%, although MgO content is relatively high (average 15 wt.%). A combination of results obtained from

field observations and study of drill-boreholes allow an estimation of 4000 tons of chromite ore. These data indicate that the Cerro Colorado ophiolite holds the promise of a source of refractory chromite in Venezuela. Such possibility needs to be further addressed in order to better define the possible existence of other chromitite bodies in the region.

8. Conclusions

• The Cerro Colorado chromitite is a podiform-like body of ophiolitic affinity, which is classified compositionally as the high-Al type (Cr#< 0.6). Major, minor and trace element fingerprints in chromite and bulk-rock PGE contents indicate that this chromitite very likely formed from a melt of tholeiitic affinity within a back-arc setting. It is suggested that the back-arc mantle experienced partial melting degrees below 20%, which were not high enough to extract significant amounts of Cr and noble metals.

• Previous age constraints of the Cerro Colorado ophiolite together with the geochemical fingerprints elucidated here for the chromitite allow to link the formation of the Cerro Colorado chromitite with the evolution of the Great Antilles Arc during Lower Cretaceous. The formation of the Cerro Colorado chromitite can be geologically linked with melts that infiltrated the mantle of a relatively mature back-arc basin originated at the rear of this intra-oceanic island arc. The Cerro Colorado high-Al chromitites, and therefore their associated ophiolitic mantle and crustal rocks, may indeed be similar to those reported in Cuba. This is a feature that should be further assessed and accounted for future palinspastic restorations for the region.

• The scientific characterization of the Cerro Colorado chromitite is also valuable from a metallogenetic point of view, revealing the existence of a source of chromite of refractory grade in Venezuela. This discovery holds the promise for new discoveries of chromium resources in the region.

Acknowledgements

References

Ahmed, A.H., Arai, S., 2002, Unexpectedly high-PGE chromitite from the deeper mantle section of the northern Oman ophiolite and its tectonics implications: Contributions to Mineralogy and Petrology, 143(3), 263–278. https://doi.org/10.1007/s00410-002-0347-8

Ahmed, A.H., Arai, S., Attia, A.K., 2001, Petrological characteristics of podiform chromitites and associated peridotites of the Pan African Proterozoic ophiolite complexes of Egypt: Mineralium Deposita, 36(1), 72–84. https://doi.org/10.1007/s001260050287

Alvarado, A., 2010, Integración geológica de la península de Araya, estado Sucre: Geos, UCV, Caracas, 40, 55-56.

Arai, S., 1997, Control of wall-rock composition on the formation of podiform chromitites as a result of magma/peridotite interaction: Resource Geology, 47, 177–187. https://doi.org/10.11456/shigenchishitsu1992.47.177

Arai, S., Miura, M., 2016, Formation and modification of chromitites in the mantle: Lithos, 264, 277–295. https://doi.org/10.1016/j.lithos.2016.08.039

Augé, T., Johan, Z., 1988, Comparative Study of Chromite Deposits from Troodos, Vourinos, North Oman and New Caledonia Ophiolites. In: Boissonnas, J., Omenetto, P. (Eds.), Mineral Deposits in the European Community: Springer-Verlag, Heidelberg, pp. 267–288. https://doi.org/10.1007/978-3-642-51858-4_15

Azer, M.K., 2013, Evolution and economic significance of listwaenites associated with Neoproterozoic ophiolites in South Eastern Desert, Egypt: Geologica Acta, 11, 113-128. https://doi.org/10.1344/105.000001777

Baquero, M., Camposano, L., Valencia, V., Grande, S., Mendi, D., Urbani, F., 2013, Petrografía, geocronología U-Pb en zircón y geoquímica de rocas máficas, península de Paraguaná, estado Falcón: Intevep, Nota Técnica NTE-1735-2013.

Barra, F., Gervilla, F., Hernández, E., Reich, M., Padrón-Navarta, J.A., 2014, Alteration patterns of chromian spinels from La Cabaña peridotite, south-central Chile: Mineralogy and Petrology, 108 (6), 819–836. https://doi.org/10.1007/s00710-014-0335-5

Baumgartner, P.O., Flores, K.E., Denyer, P., 2004, Discovery of ocean remnants in the Siuna area (NE Nicaragua): II Swiss Geoscience Meeting, Lausanne, Abstract, p. 80.

Bellizzia, A.D., Rodríguez, G., 1976, Geología del estado Yaracuy: Memorias IV Congreso Geológico Venezolano, Caracas: Boletín Geológico, 5(6), 3317-3417.

Bockrath, C., Ballhaus, C., Holzheid, A., 2004, Stabilities of laurite RuS2 and monosulphide liquid solution at magmatic temperature: Chemical Geology 208, 265–271. https://doi.org/10.1016/j.chemgeo.2004.04.016

Bonavia, F.F., Diella, V., Ferrario, A., 1993, Precambrian podiform chromitites from Kenticha Hill, southern Ethiopia: Economic Geology 88, 198–202.https://doi.org/10.2113/gsecongeo.88.1.198

Buckman, S., Ashley, P., 2010, Silica-carbonate (listwanites) related gold mineralisation associated with epithermal alteration of serpentinite bodies. New England Orogen 2010 (pp. 94-105). Armidale, NSW, Australia: University of New England.

Buisson, G., Leblanc, M., 1986, Gold bearing listwaenites (carbonatized ultramafic rocks) in ophiolite complexes. In Metallogeny of Basic and Ultramafic Rocks, ed. M.J., Gallagher, R.A. Ixer, C. R. Neary, H.M Prichard:

REFERENCES

Petrogenesis of a chromitite body from Venezuela

The Institution of Mining and Metallurgy, London, 121-132.

Bussolesi, M., Grieco, G., Tzamos, E., 2019, Olivine–Spinel Diffusivity Patterns in Chromitites and Dunites from the Finero Phlogopite-Peridotite (Ivrea-Verbano Zone, Southern Alps): Implications for the Thermal History of the Massif: Minerals. 9(2), 75. https://doi.org/10.3390/min9020075

Cáceres, J., 2016, Geología de la isla La Orchila, Dependencias Federales, Venezuela. Trabajo Especial de Grado. Universidad Central de Venezuela, Escuela de Geología, Minas y Geofísica. Inédito. 100 p.

Chan, T.K., Finch, I.J., 2001, Determination of platinum-group elements and gold by inductively coupled plasma mass spectrometry. In: Australian Platinum Conference, Perth, Western Australia, 1-9.

Colás, V., González-Jiménez, J.M., Griffin, W.L., Fanlo, I., Gervilla, F., O'Reilly, S.Y., Pearson, N.J., Kerestedjian. T., Proenza, J.A., 2014, Fingerprints of metamorphism in chromite: new insights from minor and trace elements: Chemical Geology, 389, 137-152. https://doi.org/10.1016/j.chemgeo.2014.10.001

Colás, V., Padrón-Navarta, J.A., González-Jiménez, J.M., Griffin, W.L., Fanlo, I., O'Reilly, S.Y., Gervilla, F., Proenza, J.A., Pearson, N.J., Escayola, M.P., 2016, Compositional effects on the solubility of minor and trace elements in oxide spinel minerals: insigths from cristal-crystal partition coefficients in chromite exsolution: American Mineralogist, 101(6), 1360-1372.https://doi.org/10.2138/am-2016-5611

Colás, V., González-Jiménez, J.M., Padrón-Navarta, J.A., Fanlo, I., López Sánchez-Vizcaíno, V., Castroviejo, R., Gervilla, F., 2017, Effects of silica during open-system hydrous metamorphism of chromite: Ore Geology Reviews, 90, 274–286. https://doi.org/10.1016/j.oregeorev.2017.02.025

Correa-Martínez, A.M., 2007, Petrogênese e evolução do Ofiolito de Aburrá, Cordilhera Central dos Andes Colombianos. Doctoral thesis, Universidade de Brasília. 178 p. Brasília D.F.

Dare, S.A.S., Pearce, J.A., McDonald, I., Styles, M.T., 2009, Tectonic discrimination of peridotites using fO2–Cr# and Ga–Ti–FeIII systematics in chrome-spinel: Chemical Geology, 261, 199-216. https://doi.org/10.1016/j.chemgeo.2008.08.002

Dick, H.J.B., Bullen, T., 1984, Chromian spinel as a petrogenetic indicator in abyssal and Alpine-type peridotites and spatially associated lavas: Contributions to Mineralogy and Petrology, 86(1),54–76.https://doi.org/10.1007/bf00373711

Dönmez, C., Keskin, S., Günay, K., Çolakoğlu, A.O., Çiftçi, Y., Uysal, İ., Türkel, A., Yıldırım, N., 2014, Chromite and PGE geochemistry of the Elekdağ Ophiolite (Kastamonu, Northern Turkey): Implications for deep magmatic processes in a supra-subduction zone setting: Ore Geology Reviews, 57, 216–228. https://doi.org/10.1016/j.oregeorev.2013.09.019

Economou, M., 1983, Platinum group melts in chromite ores from the Vourinos Ophiolite Complex, Greece: Ofioliti, 8, 339–356.

Economou-Eliopoulos, M., 1996, Platinum-group element distribution in chromite ores from ophiolite complexes: implications for their exploration: Ore Geology Reviews, 11(6), 363–381. https://doi.org/10.1016/s0169-1368(96)00008-x

Economou, M., Dimou, E., Economou, G., Migiros, G., Vacondios, I., Grivas, E., Rassios, A., Dabitzias, S., 1986, Chromite Deposits of Greece. In: Johan, Economou, M.(Eds.), Metallogeny of Ophiolites. UNESCO IGCP 197. Theophrastus, Athens, pp. 129–160.

Escayola, M., 2009, The point rousse listvenites, Baie Verte, Newfoundland: altered ultramafic rocks with potential for gold mineralization. In: Current Research, Newfoundland and Labrador Department of Natural Resources Geological Survey, Report 09-1, pages 1-12

Farahat, E.S., Hoinkes, G., Mogessie, A., 2011, Petrogenetic and geotectonic significance of Neoproterozoic suprasubduction mantle as revealed by theWizer ophiolite complex, Central Eastern Desert, Egypt: International Journal of Earth Sciences, 100(7), 1433–1450. https://doi.org/10.1007/s00531-010-0592-4

Farré-de-Pablo, J., Proenza, J.A., González-Jiménez, J.M., Garcia-Casco, A., Colás, V., Roqué-Rossell, J., Camprubí, A., Sánchez-Navas, A., 2019, A shallow origin for diamonds in ophiolitic chromitites: Geology, 47(1), 75-78. https://doi.org/10.1130/g45640.1

Ferreira-Filho, C.F., Marques, J.C., Spier, C.A., Araújo, S.M., Porto, F.S., 2002, Review of Brazilian chromite deposits associated with layered complexes: constraints for the postulated genetic models. In 9th Platinum symposium abstracts.

Flores, K., Baumgartner, P.O., Skora, S., Baumgartner, L., Muntener, O., Cosca, M., Cruz, D., 2007, The Siuna Serpentinite Melange: An Early Cretaceous Subduction/Accretion of a Jurassic Arc: American Geophysical Union, Fall Meeting 2007, abstract #T11D-03.

Fonseca, R.O.C., Brückel, K., Bragagni, A., Leitzke, F.P., Speelmanns, I.M., Wainwright, A.N., 2017, Fractionation of Rhenium from Osmium during noble metal alloy formation in association with sulfides: Implications for the interpretation of model ages in alloy-bearing magmatic rocks: Geochimica et Cosmochimica Acta, 216, 184-200. https://doi.org/10.1016/j.gca.2017.04.041

Fonseca, R.O.C., Laurenz, V., Mallmann, G., Luguet, A., Hoehne, N., Jochum, K.P., 2012, New constraints on the genesis and long-term stability of Os-rich alloys in the Earth's mantle: Geochimica et Cosmochimica Acta, 87, 227–242. https://doi.org/10.1016/j.gca.2012.04.002

Franco, A., Torrealba, N., 1987, Rocas ultramáficas de Paraguaná y mineralizaciones asociadas: Ministerio de Energía y Minas, Venezuela. Inédito, 38 p.

Gao, S., Liu, X., Yuan, H., Hattendorf, B., Günther, D., Chen, L., and Hu, S., 2002, Determination of forty two major and trace elements in USGS and NIST SRM glasses by laser ablation-inductively coupled plasma-mass spectrometry: Geostandards Newsletter, 26(2), 181–196. https://doi.org/10.1111/j.1751-908x.2002.tb00886.x

Garuti, G., Pushkarev, E., Zaccarini, F., 2005, Diversity of chromite-PGE mineralization in ultramafic complexes of the Urals. In: Törmänen, T.O., Alapieti, T.T. (Eds.), Platinum-group elements—from genesis to beneficiation and environmental impact. Tenth Int. Platinum Symp. (Oulu), pp. 341–344.

Gervilla, F., Proenza, J.A., Frei, R., González-Jiménez, J.M., Garrido, C., Melgarejo, J.C., Meibom, A., Díaz-Martínez, R., Lavaut, W., 2005, Distribution of platinum-group elements and Os isotopes in chromite ores from Mayarí–Baracoa Ophiolitic Belt (eastern Cuba): Contributions to Mineralogy and Petrology, 150(6), 589–607. https://doi.org/10.1007/s00410-005-0039-2

Giunta G., Beccaluva, L., Coltorti, M., Siena, F., Vaccaro, C, 2002, The southern margin of the Caribbean Plate in Venezuela: tectono-magmatic setting of the ophiolitic units and kinematic evolution. Lithos, 63(1-2), 19-40. https://doi.org/10.1016/s0024-4937(02)00120-2

González-Jiménez, J.M., Proenza, J.A., Gervilla, F., Melgarejo, J.C., Blanco-Moreno, J.A., Ruiz- Sánchez, R., 2011a, High-Cr- and Al-rich chromitites from Sagua de Tánamo chromite district, Mayarí-Cristal Ophiolitic Massif (eastern Cuba): mineralogy and geochemistry of the platinum-group elements: Lithos,125, 101–121. https://doi.org/10.1016/j.lithos.2011.01.016

González-Jiménez, J.M., Augé, T., Gervilla, F., Bailly, L., Proenza, J.A., Griffin, B., 2011b, Mineralogy and geochemistry of

platinum-rich chromitites from the mantle–crust transition zone at Ouen Island, New Caledonia ophiolite: Canadian Mineralogist, 49(6), 1549–1570. https://doi.org/10.3749/canmin.49.6.1549

González-Jiménez, J.M., Griffin, W.L., Proenza, J.A., Gervilla, F., O'Reilly, S.Y., Akbulut, M., Pearson, N.J., Arai, S., 2014, Chromitites in ophiolites: How, where, when, why? Part II. The crystallization of chromitites. Lithos. http://dx.doi.org/10.1016/j.lithos.2013.09.008.

González-Jiménez, J.M., Locmelis, M., Belousova, E., Griffin, William L., Gervilla, F., Kerestedjian, T., O'Reilly, S.Y., Sergeeva, I., Pearson, N.J., 2015, Genesis and tectonic implications of podiform chromitites in the metamorphosed Ultramafic Massif of Dobromirtsi (Bulgaria): Gondwana Research, 27(2), 555–574. https://doi.org/10.1016/j.gr.2013.09.020

González-Jiménez, J.M., Barra, F., Garrido, L.N.F., Reich, M., Satsukawa, T., Romero, R., Salazar, E., Colás, V., Orellana, F., Rabbia, O., Plissart, G., Morata, D., 2016, A secondary precious and base metal mineralization in chromitites linked to the development of a Paleozoic accretionary complex in Central Chile: Ore Geology Reviews, 78, 14–40. https://doi.org/10.1016/j.oregeorev.2016.02.017

González-Jiménez, J.M., Proenza, J.A., Martini M., Camprubí, A., Griffin, W.L., O'Reilly S.Y., Pearson, N.J., 2017a, Deposits associated with ultramafic-mafic complexes in Mexico: the Loma Baya case. Ore Geology Reviews, 81, 1053-1065. https://doi.org/10.1016/j.oregeorev.2015.05.014

González-Jiménez, J.M., Camprubí, A., Colás, V., Griffin, W.L., Proenza, J.A., O'Reilly, S.Y., Centeno-García, E., García-Casco, A., Belousova, E., Talavera, C., Farré-de-Pablo, J., Satsukawa, T., 2017b, The recycling of chromitites in ophiolites from southwestern North America: Lithos, 294-295, 53-72. https://doi.org/10.1016/j.lithos.2017.09.020

Graham, I.T., Franklin, B.J., Marshall, B., 1996, Chemistry and mineralogy of podiform chromitite deposits, southern NSW, Australia: a guide to their origin and evolution: Mineralogy and Petrology, 57, 129–150. https://doi.org/10.1007/bf01162355

Hickey, R.L., Frey, F.A., 1982, Geochemical characteristics of boninite series volcanics; implications for their source: Geochimica et Cosmochimica Acta, 46(11), 2099-2116. https://doi.org/10.1016/0016-7037(82)90188-0

Iturralde-Vinent, M., Díaz-Otero, C., Rodríguez-Vega, A., Díaz-Martínez, R., 2006, Tectonic implications of paleontologic dating of Cretaceous-Danian sections of Eastern Cuba: Geologica Acta, 4, 89-102. https://doi.org/10.1344/105.000000359

Jochum, K.P., Weis, U., Stoll, B., Kuzmin, D., Yang, Q., Raczek, I., Jacob, D.R., Stracke, A., Birbaum, K., Frick, D.A., Günther, D., Enzweiler, J., 2011, Determination of reference values for Nist SRM 610-617 glasses following ISO guidelines: Geostandards and Geoanalytical Research, 35(4), 297-429. https://doi.org/10.1111/j.1751-908x.2011.00120.x

Kamenetsky, V.S., Crawford, A.J., Meffre, S., 2001, Factors controlling chemistry of magmatic spinel: an empirical study of associated olivine, Cr-spinel and melt inclusions from primitive rocks: Journal of Petrology, 42(4), 655–671. https://doi.org/10.1093/petrology/42.4.655

Kerr, A., Neill, I., Urbani, F., Spikings, R., Barry, T., Tarney, J., 2012, The Siquisique basalts and gabbros, Los Algodones, Venezuela: Late Cretaceous oceanic plateau formed within the proto-Caribbean plate?: Geos, UCV, Caracas, 42, 146.

Kocks, H., Melcher, F., Meisel, T., Burgath, K.P., 2007, Diverse contributing sources to chromitite petrogenesis in the Shebenik

Ophiolitic Complex, Albania: evidence from new PGE- and Os-isotope data: Mineralogy and Petrology, 91(3-4),139–170. https://doi.org/10.1007/s00710-007-0194-4

Latypov, R., Chistyakova, S., Mukherjee, R., 2017, A novel hypothesis for origin of massive chromitites in the Bushveld igneous complex: Journal of Petrology, 58, 1899-1940. https://doi.org/10.1093/petrology/egx077

Leblanc, M., Nicolas, A., 1992, Les chromitites ophiolitiques: Chronicles Recherche Minière, 507, 3–25.

Leblanc, M., 1995, Chromite and ultramafic rock compositional zoning through a paleotransform fault, Poum, New Caledonia: Economic Geology, 90(7), 2028–2039. https://doi.org/10.2113/gsecongeo.90.7.2028

Lewis J.F., Draper, G., Proenza, J.A. Espaillat, J., Jiménez. J., 2006, Ophiolite-Related Ultramafic Rocks (Serpentinites) in the Caribbean Region: A Review of their Occurrence, Composition, Origin, Emplacement and Ni-Laterite Soil Formation: Geologica Acta, 4 (1-2), 237-263. https://doi.org/10.1344/105.000000368

Luguet, A., Reisberg, L., 2016, Highly Siderophile Element and 187Os Signatures in Non-cratonic Basalt-hosted Peridotite Xenoliths: Unravelling the Origin and Evolution of the Post-Archean Lithospheric Mantle: Reviews in Mineralogy and Geochemistry, 81(1), 305-367. https://doi.org/10.2138/rmg.2016.81.06

Malitch, K.N., Melcher, F. and Mühlans, H.W., 2001, Palladium and gold mineralization in podiform chromitites at Kraubath, Austria: Mineralium Deposita, 73(4), 247–277. https://doi.org/10.1007/s007100170002

Mallmann, G., O'Neill, H.St.C., 2009, The crystal/melt partitioning of V during mantle melting as function of oxygen fugacity compared with some other elements (Al, P, Ca, Sc, Ti, Cr, Fe, Ga, Y, Zr and Nb: Journal of Petrology, 50(9), 1765-1794. https://doi.org/10.1093/petrology/egp053

Marchesi, G., González-Jiménez, J.M., Gervilla, F., Garrido, C.J., Griffin, W.L., O'Reilly, S.Y., Proenza, J.A., Pearson, N.J., 2011, *In situ* Re–Os isotopic analysis of platinum-group minerals from the Mayarí–Cristal ophiolitic massif (Mayarí–Baracoa Ophiolitic Belt, eastern Cuba): implications for the origin of Os-isotope heterogeneities in podiform chromitites: Contributions to Mineralogy and Petrology, 161(6), 977–990. https://doi.org/10.1007/s00410-010-0575-2

Maresch, W.V., Kluge, R., Baumann, A., Pindell, J.L., Krückhans-Lueder, G., Stanek, K., 2009, The occurrence and timing of high-pressure metamorphism on Margarita Island, Venezuela: a constraint on Caribbean-South America interaction: Geological Society, London, Special Publications, 328(1), 705-741. https://doi.org/10.1144/sp328.28

Martín-Bellizzia, C., 1960, Estudio petrográfico de las rocas procedentes de los cerros El Rodeo, Tausabana y Santa Ana. In: Memorias del III Congerso Geológico Venezolano: Boletín de Geología. (Caracas) 3(4), 729-743.

Mathez, E.A., Kinzler, R.J., 2017, Metasomatic chromitite seams in the Bushveld and Rum Intrusions: Elements, 13(6), 397-402. https://doi.org/10.2138/gselements.13.6.397

Maurel, C., Maurel, P., 1982, Étude expérimentale de la distribution de l'aluminium entre bain silicaté basique et spinelle chromifère. Implications pétrogénétiques: teneur en chrome des spinelles: Bulletin du Mineralógie, 105, 197–202.

McElduff, B., Stumpfl, E.F., 1991, The chromite deposits of the Troodos Complex, Cyprus — evidence for the role of a fluid phase accompanying chromite formation: Mineralium Deposita, 26(4), 307–318. https://doi.org/10.1007/bf00191079

Melcher, F., Stumpfl, E.F., Distler, V., 1994, Chromite deposits of the Kempirsai massif,

southern Urals, Kazakhstan: Applied Earth Section B (Transactions Institution Mining and Metallurgy) 103, B87–B162.

Melcher, F., Grum, W., Simon, G., Thalhammer, T.V., Stumpfl, E.F., 1997, Petrogenesis of the ophiolitic giant chromite deposits of Kempirsai, Kazakhstan: a study of solid and fluid inclusions in chromite: Journal of Petrology, 38(10), 1419–1458. https://doi.org/10.1093/petrology/38.10.1419

Melcher, F., Grun, W., Thalhammer, T.V., Thalhammer, O.A.R., 1999, The giant chromite deposits at Kempirsai, Urals: constraints from trace elements (PGE, REE) and isotope data: Mineralium Deposita, 34(3), 250–272. https://doi.org/10.1007/s001260050202

Méndez, J., 1960, La cromita de Paraguaná, Estado Falcón: In: Memorias del III Congreso Geologico Venezolano: Boletín de Geología. (Caracas) 3(4), 718-728.

Mendi, D., Rodríguez. E., 2006, Integración geológica de la península de Paraguaná, estado Falcón: Geos, UCV, Caracas, 38, 93-94.

Mistage, M., 1989, Estudio Geológico de los Cuerpos Ultramáficos del Macizo de Santa Ana, Península de Paraguaná, Estado Falcón. Trabajo Especial de Grado. Universidad Central de Venezuela, Escuela de Geología, Minas y Geofísica. Inédito. 97 p.

Mistage, M., Urbani, F., Franco, A., 1989, Geología de los cuerpos ultramáficos de los cerros El Rodeo y Arajó, península de Paraguaná Estado Falcón: Memorias VII Congreso Geologico Venezolano.

Morishita, T., Dilek, Y., Shallo,M., Tamura, A., Arai, S., 2011, Insight into the uppermost mantle section of a maturing arc: the Eastern Mirdita ophiolite, Albania: Lithos 124, 215–226. https://doi.org/10.1016/j.lithos.2010.10.003

Mudd, G.M., Jowitt, S., Werner, T., 2018, Global platinum group element resources, reserves and mining–a critical assessment: Science of the Total Environment, 622-623, 614-625. https://doi.org/10.1016/j.scitotenv.2017.11.350

Mudholkar, A., Paropkari, A.L., 1999, Evolution of the basalts from three back-arc basins of southwest Pacific: Geo-Mar Letters, 18, 305–314. https://doi.org/10.1007/s003670050084

Mukherjee, R., Mondal, S.K., Rosing, M.T., Frei, R., 2010, Compositional variations in the Mesoarchean chromites of the Nuggihalli schist belt, Western Dharwar Craton (India): potential parental melts and implications for tectonic setting: Contributions to Mineralogy and Petrology, 160 (6), 865–885. https://doi.org/10.1007/s00410-010-0511-5

Mukherjee, R., Latypov, R. & Balakrishnan, A., 2017, An intrusive origin of some UG-1 chromitite layers in the Bushveld Igneous Complex, South Africa: insights from field relationships: Ore Geology Reviews, 90, 94–109. https://doi.org/10.1016/j.oregeorev.2017.03.008

Naldrett, A.J., Duke, J.M., 1980, Pt metals in magmatic sulfide ores: Science 208, 1417–1424. https://doi.org/10.1126/science.208.4451.1417

Naldrett, A.J., Wilson, A., Kinnaird, J., Yudovskaya, M., Chunnett, G., 2012, The origin of chromitites and related PGE mineralization in the Bushveld Complex: new mineralogical and petrological constraints: Mineralium Deposita, 47 (3), 209–232. https://doi.org/10.1007/s00126-011-0366-3

Norman, M., Pearson, N., Sharma, A., Griffin, W., 1996, Quantitative analysis of trace elements in geological materials by laser ablation ICPMS: Instrumental operating conditions and calibration values of NIST glasses: Geostandards Newsletter, 20, 247–261. https://doi.org/10.1111/j.1751-908X.1996.tb00186.x

O'Driscoll, B., González-Jiménez, J.M., 2016, Petrogenesis of the platinum-group minerals: Reviews in Mineralogy and Geochemistry,

81(1), 489–578. https://doi.org/10.2138/rmg.2016.81.09

O'Driscoll, B., VanTongeren, J. A., 2017, Layered intrusions: from petrological paradigms to precious metal repositories: Elements, 13(6), 383–389. https://doi.org/10.2138/gselements.13.6.383

Pagé, P., Barnes, S.-J., 2009, Using trace elements in chromites to constrain the origin of podiform chromitites in the Thetford Mines ophiolite, Québec, Canada: Economic Geology, 104(7), 997–1018. https://doi.org/10.2113/gsecongeo.104.7.997

Parkinson, I.J., Arculus, R.J., 1999, The redox state of subduction zones: insights from arc-peridotites: Chemical Geology, 160(4), 409-423. https://doi.org/10.1016/s0009-2541(99)00110-2

Paton, C., Hellstrom, J., Paul, B., Woodhead, J., Hergt, J., 2011, Iolite: freeware for the visualization and processing of mass spectrometric data: Journal of Analytical Atomic Spectrometry, 26(12), 2508-2512. https://doi.org/10.1039/c1ja10172b

Peng, G., Lewis, J., Lipin, B., McGee, J., Bao, P., Wang, X., 1995, Inclusions of phlogopite and phlogopite hydrates in chromite from the Hongguleleng ophiolite in Xinjang, northwest China: American Mineralogist, 80, 1307–1316. https://doi.org/10.2138/am-1995-11-1221

Petrásh, D., Revanales., C., 2010, Integración geológica de la península de Paria, estado Sucre: Geos, UCV, Caracas, 40, 68-70.

Pindell, J.L., Maresch, W.V., Martens, U., Stanek, K.P., 2012, The greater antillean arc: early Cretaceous origin and proposed relationship to Central American subduction mélanges: implications for models of Caribbean evolution: International Geology Review 54(2), 131-143. https://doi.org/10.1080/00206814.2010.510008

Pouchou, J.L., Pichoir, F. 1985, Quantitative analysis of homogeneous or stratified microvolumes applying the model PAP. In

Electron Probe Quantitation; Heinrich, K.J., Newbury, D.E., Eds.; Plenum Press: New York, USA, 1991, pp. 31–75.

Prichard, H.M., Neary, C.R., Fisher, F.C., O'Hara, M.J., 2008, PGE-rich Podiform chromitites in the Al'Ays ophiolite complex, Saudi Arabia: an example of critical mantle melting to extract and concentrate PGE: Economic Geology, 103(7), 1507–1529. https://doi.org/10.2113/gsecongeo.103.7.1507

Proenza, J.A., Gervilla, F., Melgarejo, J.C., Bodinier, J.L., 1999, Al- and Cr-rich chromitites from the Mayarí–Baracoa Ophiolitic Belt (eastern Cuba): consequence of interaction between volatile-rich melts and peridotite in suprasubduction mantle: Economic Geology, 94(4), 547–566. https://doi.org/10.2113/gsecongeo.94.4.547

Proenza, J.A., Ortega-Gutiérrez, F., Camprubí, A., Tritlla, J., Elías-Herrera, M., Reyes-Salas, M., 2004a, Paleozoic serpentinite-enclosed chromitites from Tehuitzingo (Acatlan complex, southern Mexico): a petrological and mineralogical study: Journal of South American Earth Sciences, 16(8), 649–666. https://doi.org/10.1016/j.jsames.2003.12.003

Proenza, J.A., Escayola, M., Ortiz, F., Pereira, E., Correa, A.M., 2004b, Dunite and associated chromitites from Medellín (Colombia). In: 32nd International Geological Congress, pt 1, abs 1-1: 507 p.

Proenza, J.A., Zaccarini, F., Lewis, J.F., Longo, F., Garuti, G., 2007, Chromian spinel composition and the platinum-group minerals of the PGE-rich Loma Peguera chromitites, Loma Caribe peridotite, Dominican Republic: The Canadian Mineralogist, 45(3), 631–648. https://doi.org/10.2113/gscanmin.45.3.631

Proenza, J.A., Zaccarini, F., Escayola,M., Cábana, C., Schalamuk, A., Garuti, G., 2008, Composition and textures of chromite and platinum-group minerals in chromitites of the western ophiolitic belt from Córdoba

Pampean Ranges, Argentine: Ore Geology Reviews, 33(1), 32–48. https://doi.org/10.1016/j.oregeorev.2006.05.009

Proenza, J.A., González-Jiménez, J.M.,García-Casco, A., Belousova, E., Griffin, W.L., Talavera, C., Rojas-Agramonte, Y., Aiglsperger, T., Navarro-Ciruana, D., Pujol-Solà, N., Gervilla, F., O'Reilly, S.Y., Jacob, D.E., 2018, Cold plumes trigger contamination of oceanic mantle wedges with continental crust-derived sediments: Evidence from chromitite zircon grains of eastern Cuban ophiolites: Geoscience Frontiers, 9(6), 1921-1936. https://doi.org/10.1016/j.gsf.2017.12.005

Pujol-Solà, N., Proenza, J.A., García-Casco, A., González-Jiménez, J.M., Andreazini, A., Melgarejo, J.C., Gervilla, F., 2018, An alternative scenario on the origin of ultra-high pressure (UHP) and super-reduced (SuR) minerals in ophiolitic chromitites: a case study from the Mercedita Deposit (eastern Cuba): Minerals, 8(10), 433. https://doi.org/10.3390/min8100433

Rammlmair, D., Raschka, H., Steiner, L., 1987, Systematics of chromitite occurrences in Central Palawan, Philippines: Mineralium Deposita, 22(3), 190–197. https://doi.org/10.1007/bf00206609

Rekowski, F., Rivas, L., 2006, Integración geológica de la isla de Margarita, estado Nueva Esparta: Geos, UCV, Caracas, 38:97-98.

Rodríguez, H., Muñoz, P., 2009, Geología de las unidades ígneas y sedimentarias de Siquisique-Puente Limón, estado Lara: Geos, UCV, Caracas, 40. 68-69.

Rojas-Agramonte, Y., Garcia-Casco, A., Kemp, A., Kröner, A., Proenza, J.A., Lázaro, C. Liu, D., 2016, Recycling and transport of continental material through the mantle wedge above subduction zones: A Caribbean example: Earth and Planetary Science Letters, 436, 93–107. https://doi.org/10.1016/j.epsl.2015.11.040

Rollinson, H., 2005, Chromite in the mantle section of the Oman ophiolite: a new genetic model: The Island Arc, 14(4), 542–550. https://doi.org/10.1111/j.1440-1738.2005.00482.x

Rollinson, H., 2008, The geochemistry of mantle chromitites from the northern part of the Oman ophiolite: inferred parental melt compositions: Contributions to Mineralogy and Petrology, 156(3), 273–288. https://doi.org/10.1007/s00410-008-0284-2

Rollinson, H., 2016, Surprises from the top of the mantle transition zone: Geology Today, 32(2) 58-64. https://doi.org/10.1111/gto.12130

Santamaría, F., Schubert., C., 1974, Geochemistry and geochronology of the Southern Caribbean-Northern Venezuela plate boundary: Bulletin of the Geological Society of America, 85(7), 1085-1098. https://doi.org/10.1130/0016-7606(1974)85<1085:gagots>2.0.co;2

Sisson, V.B., Ertan, I.E., Ave-Lallemant, H.G., 1997, High pressure (~2000 MPa) kyanite and glaucophane-bearing pelitic schist and eclogite from Cordillera de la Costa belt, Venezuela: Journal of Petrology, 38(1), 65-83. https://doi.org/10.1093/petrology/38.1.65

Tarkian, M., Nadienova, E., Zhelyaskova-Panayotova, M., 1991, Platinum-group minerals in chromitites from the eastern Rhodope ultramafic complex, Bulgaria: Mineralogy and Petrology, 44, 73–87. https://doi.org/10.1007/bf01167101

Tassinari, C.C.G., Castroviejo, R., Rodrigues, J.F., Acosta, J., Pereira, E., 2011, A Neoproterozoic age for the chromitite and gabbro of the Tapo ultramafic Massif, Eastern Cordillera, Central Peru and its tectonic implications: Journal of South American Earth Sciences, 32 (4), 429–437. https://doi.org/10.1016/j.jsames.2011.03.008

Thalhammer, O.A.R., Prochaska, W., Mühlhans, H.W., 1990, Solid inclusions in chrome-spinels and platinum group element concentration from the Hochgrössen and Kraubath Ultramafic Massifs (Austria): Contributions to Mineralogy and Petrology, 105(1), 66–80. https://doi.org/10.1007/bf00320967

Thayer, T.P., 1946, Preliminary chemical correlation of chromite with the containing rocks: Economic Geology, 41(3), 202-217. https://doi.org/10.2113/gsecongeo.41.3.202

Urbani, F., 2018, Una revisión de los terrenos geológicos del Sistema Montañoso del Caribe, norte de Venezuela: Boletín de Geología, Caracas, 36. 117-216.

Uysal, I., Tarkian, M., Sadiklar, M.B., Zaccarini, F., Meisel, T., Garuti, G., Heidrich, S., 2009, Petrology of Al- and Cr-rich ophiolitic chromitites from the Muğla, SW Turkey: implications from composition of chromite, solid inclusions of platinum-group mineral, silicate, and base-metal mineral, and Os-isotope geochemistry: Contributions to Mineralogy and Petrology, 158(5), 659–674. https://doi.org/10.1007/s00410-009-0402-9

Vatin-Perignon, N., Amossé, J., Radelli, L., Keller, F., Castro-Leyva, T., 2000, Platinum group element behaviour and thermochemical constraints in the ultrabasic–basic complex of the Vizcaino Peninsula, Baja California Sur, Mexico: Lithos, 53(1), 59–80. https://doi.org/10.1016/s0024-4937(00)00006-2

Wasylenki, L.E., Baker, M.B., Kent, A.J.R., Stolper, E.M., 2003, Near solidus melting of the shallow upper mantle: partial melting experiments on depleted peridotite: Journal of Petrology, 44(7), 1163–1191. https://doi.org/10.1093/petrology/44.7.1163

Wilson, M., 1989, Igneous petrogenesis. Unwin Hyman, London.

Yang, K., Seccombe, P., 1993, Platinum-group minerals in the chromitites from the Great Serpentinite Belt, NSW, Australia: Mineralogy and Petrology, 47(2-4), 263-286. https://doi.org/10.1007/bf01161571

Yao, S., 1999, Chemical composition of chromites from ultramafic rocks: application to mineral exploration and petrogenesis. (PhD thesis) Macquarie University, Sydney (174 pp.).

Zaccarini, F., Garuti, G., Proenza, J.A., Campos, L., Thalhammer, O.A.R., Aiglsperger, T., Lewis, J., 2011, Chromite and platinum-group-elements mineralization in the Santa Elena ophiolitic ultramafic nappe (Costa Rica): geodynamic implications: Geologica Acta, 9, 407–423. https://doi.org/10.1344/105.000001696

Zhou, M.F., Bai, W.J., 1992, Chromite deposits in China and their origin: Mineralium Deposita, 27(3), 192–199. https://doi.org/10.1007/bf00202542

Zhou, M.F., Robinson, P.T., 1994, High-Cr and high-Al podiform chromitites, Western China: relationships to partial melting and melt/rock reaction in the upper mantle: International Geology Review 36(7), 678–686. tps://doi.org/10.1080/00206819409465481

Zhou, M.F., Robinson, P.T., Bai, W.J., 1994, Formation of podiforme chromites bymelt–rock interaction in the upper mantle: Mineralium Deposita, 29(1), 98–101. https://doi.org/10.1007/bf03326400

Zhou, M.F., Robinson, P.T., Malpas, J., Zijin, L., 1996, Podiform chromites in the Luobusa Ophiolite (Southern Tibet): implications for melt–rock interaction and chromite segregation in the upper mantle: Journal of Petrology, 37(1), 3–21. https://doi.org/10.1093/petrology/37.1.3.